

A review of thermal and water management in polymer electrolyte membrane fuel cells

Vinodkumar.E¹, Dr. Manojkumr.P², Dr. M.R.Radhakrishnapanicker³

¹(Associate professor, SNGCE)

²(Associate professor, PSG TECH, Coimbatore)

³(Professor, Division of Mechanical Engineering, CUSAT)

Abstract: Polymer electrolyte membrane (PEM) fuel cells, which convert the chemical energy stored in hydrogen fuel directly and efficiently to electrical energy with water as the only byproduct, have the potential to reduce our energy use, pollutant emissions, and dependence on fossil fuels. Great deal of efforts has been made in the past, particularly during the last couple of decades or so, to advance the PEM fuel cell technology and fundamental research. In this regard, fundamental studies play an important and indeed critical role. Issues such as water and heat management, and new material development remain the focus of fuel-cell performance improvement and cost reduction. The objective of this review is three folds: (1) to present the latest status of PEM fuel cell technology development and applications in the transportation, stationary, and portable/micro power generation sectors through an overview of the state-of-the-art and most recent technical progress; (2) to describe the need for fundamental research in this field and fill the gap of addressing the role of fundamental research in fuel cell technology; and (3) to outline major challenges in fuel cell technology development and the needs for fundamental research for the near future and prior to fuel cell commercialization.

Key words: Nafion, Cell potential, Platinum catalyst, Membrane electrode assembly, polarisation curve, water transport, heat convection

I. Introduction

Due to the growing concerns on the depletion of petroleum-based energy resources and climate change, fuel cell technologies have received much attention in recent years owing to their high efficiencies and low emissions. Fuel cells, which are classified according to the electrolyte employed, are electrochemical devices that directly convert chemical energy stored in fuels such as hydrogen to electrical energy. Its efficiency can reach as high as 60% in electrical energy conversion and overall 80% in co-generation of electrical and thermal energies with >90% reduction in major pollutants [1]. Five categories of fuel cells have received major efforts of research: (1) polymer electrolyte membrane (PEM) fuel cells or PEMFCs (also called PEFCs), (2) solid oxide fuel cells (SOFCs), (3) alkaline fuel cells (AFCs), (4) phosphoric acid fuel cells (PAFCs), and (5) molten carbonate fuel cells (MCFCs). PEM fuel cells are constructed using polymer electrolyte membranes (notably Nafion) as proton conductor and Platinum (Pt)-based materials as catalyst. Their noteworthy features include low operating temperature, high power density, and easy scale-up, making PEM fuel cells a promising candidate as the next generation power sources for transportation, stationary, and portable applications. Fig. 1 shows a schematic of a PEM fuel cell. The very first fuel cell was invented in 1839 by Sir William Robert Grove (an English lawyer turned scientist), though no practical use was found for another century [2]. General Electric Company (GE) began developing fuel cells in the 1950s and was awarded the contract for the Gemini space mission in 1962. The 1 kW Gemini fuel cell system had a platinum loading of 35 mg Pt/cm² and performance of 37 mA/cm² at 0.78 V [3]. In the 1960s improvements were made by incorporating Teflon in the catalyst layer directly adjacent to the electrolyte, as was done with GE fuel cell at the time. Considerable improvements were made from the early 1970s onward with the adoption of the fully fluorinated Nafion membrane. Though many technical and associated fundamental breakthroughs have been achieved during the last couple of decades, many challenges such as reducing cost and improving durability while maintaining performance remain prior to the commercialization of PEM fuel cells. In the remaining of this section, the current status of PEM fuel cell technology and applications are first presented, follow by discussions on commercialization barriers and the role of fundamental research.

At the stack level, water and heat management becomes more complex due to the interactions of constituent sub-cells. Individual cells communicate in many ways in a stack. One is the electrical connection, i.e. the electrical current flows through all the individual cells in a series stack, therefore a local high electronic resistance will significantly affect the stack performance.

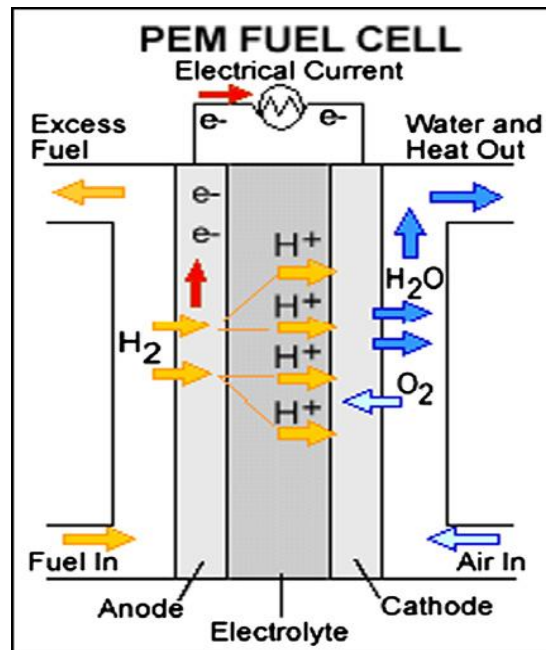


Fig.1 Schematic of a PEM fuel cell

1.1 Applications of PEM fuel cell technology and its current status

The major application of PEM fuel cells focuses on transportation primarily because of their potential impact on the environment, e.g. the control of emission of the greenhouse gases (GHG). Other applications include distributed/stationary and portable power generation. Most major motor companies work solely on PEM fuel cells due to their high power density and excellent dynamic characteristics as compared with other types of fuel cells. Fuel-cell vehicles (FCV) have been developed and demonstrated, e.g. GM Hydrogen 1, Ford Demo Ila (Focus), DaimlerChrysler NeCar4a, Honda FCX-V3, Toyota FCHV, Nissan XTERRA FCV, VW Bora HyMotion, and Hyundai Santa Fe FCV. Auto makers such as Toyota, Honda, Hyundai, Daimler, and General Motors (GM) have announced plans of commercializing their fuel-cell vehicles by 2015 [4]. Distributed PEM fuel cell power system is primarily focused on small scale (50–250 kW for decentralized use or <10 kW for households) [5]. The high cost of PEM fuel cells remains a major barrier that prohibits their widespread applications in this area. Back-up power for banks and telecommunication companies receives growing interests recently because of the extremely high cost associated with power breakdowns. Another promising area is portable power supply, considering that limited energy capacity of batteries unlikely meets the fast-growing energy demand of the modern portable electric devices such as laptops, cell phones and military radio/communication devices. PEM fuel cells provide continuous power as long as hydrogen fuel is available and they can be fabricated in small sizes without efficiency loss. Fig 1. Major electronics companies, such as Toshiba, Sony, Motorola, LG, and Samsung, have in-house R&D units for portable fuel cells.

1.2 Commercialization barriers

The two greatest barriers are durability and cost. Fuel cell components, such as the MEA (membrane electrode assembly) [6], suffer degradation during long-term operations. The lifetime required by a commercial fuel cell is over 5000 operating hours for light-weight vehicles and over 40,000 h for stationary power generation with less than a 10% performance decay [7,8]. At current, most fuel cells exhibit major performance decay after around a thousand hours of operation [7,9,10]. One primary portion of a fuel cell cost is due to the MEA that consists of a Nafion membrane and catalyst (usually Pt-based) layers [11]. The Pt loading has been reduced by two orders of magnitude in the past decade and there is still room for further loading reduction. The 2010 and 2015 DOE targets for the fuel cell cost is \$45/kW and \$30/kW, respectively, for transportation applications [1,17]. Fig. 2 shows the breakdown of fuel cell cost.

1.3 The role of fundamental research

Various interrelated and complex phenomena occur during fuel cell operation, including mass/heat transfer, electrochemical reactions, and ionic/electronic transport, which govern fuel cell operation. Further scientific breakthroughs are required to overcome barriers related to cost and durability to enable fuel cell commercialization. Breakthroughs in material development, acquisition of fundamental knowledge, and development of analytical models and experimental tools are particularly important for current fuel cell development [6]. For example, avoiding electrode flooding is of critical importance for optimal fuel-cell performance and durability; however this phenomenon is not well understood. The ability to model fuel and reactant transport and electrochemical reactions in electrodes is critical, particularly in the cathode in which the oxygen reduction reaction (ORR) is sluggish and inefficient and water is generated. This review focuses on discussing PEMFC application, technology status, and the needs on fundamental research. PEM fuel cells are being applied in the following three areas: transportation, stationary, and portable power generation. The power of electric passenger car, utility vehicles, and bus ranges from 20 kW to 250 kW. The stationary power by general fuel cells has a wide range, 1–50 MW. Some small-scale stationary generation, e.g. for the remote telecommunication application, is 100–1 kW [12].

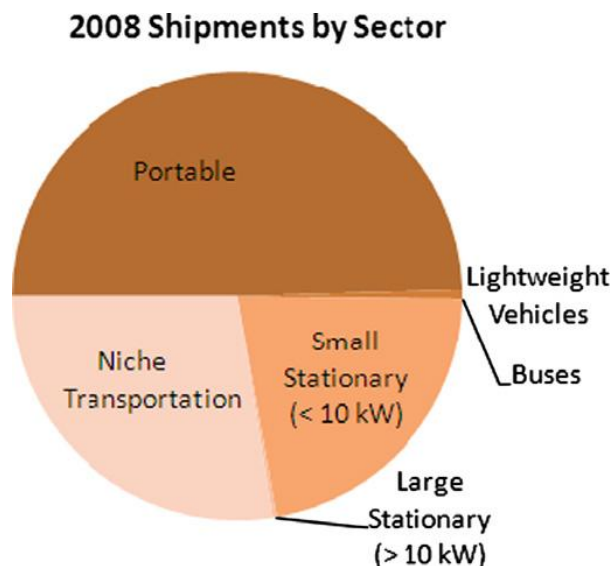


Fig.2. PEM fuel cell units installed around the world in each category

The portable power is usually in the range of 5–50 W. Fig. 2 displays the portion of PEM fuel cell units installed around the world in each category in 2008.

II. Transportation and other applications

Several concerns arise from the global, fast-growing vehicle market, such as air pollution, climate change (due to the greenhouse gases), and fuel sustainability. Most issues are associated with the conventional engines, i.e. ICEs (internal-combustion engines), which primarily depend on hydrocarbon fuels. PEM fuel cells have the potential to replace ICEs due to their potentials of achieving higher efficiency and lower GHG emissions. The typical power range for this type of applications, such as passenger cars, utility vehicles, and buses, ranges from 20 kW to 250 kW. Interests in fuel-cell vehicles can be traced back to the late 1970s and received a major boost in recent years. The technology roadmap published by Ballard Power Systems discussed several main challenges for fuel-cell vehicles: durability, cost and freeze-start [13].

2.1.1 Light-weight vehicles

Fig.3 shows that the production of regular automobiles working on PEMFC increases steadily in early 2000s but becomes fluctuated in recent years. In the past few years, the fuel cell light-weight vehicle market has been led by Honda, General Motors, and others. Honda has started shipping its FCX Clarity, to Southern and Northern California since these regions are now equipped with hydrogen fuelling stations, where the FCX

Clarity is offered to selected customers for a 3-year lease at \$600/month. Table 1 documents the key parameters of several fuel-cell vehicles.

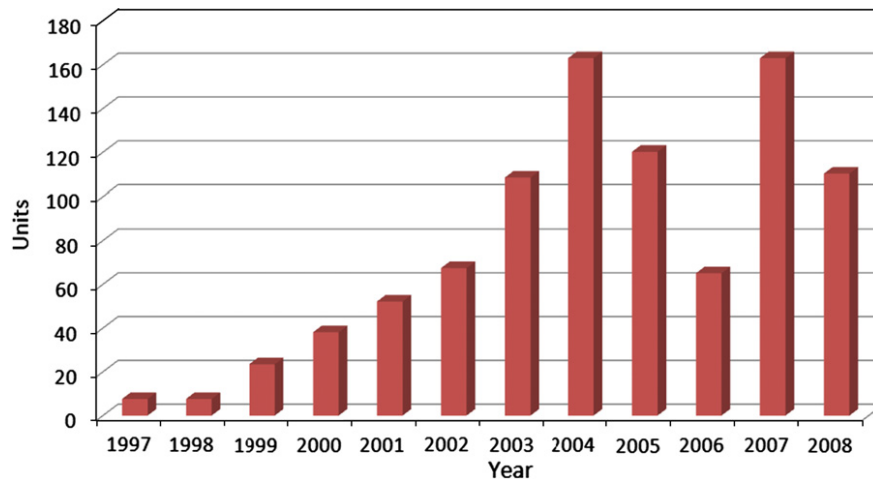


Fig.3 Production of regular automobiles using PEMFCs.

Table 1
 Specifications of several fuel-cell vehicles [265,286–293] (for a more complete listing of fuel-cell vehicles, see Ref. [294]).

Vehicle name	Type	Year	Power (kW)	Hydrogen storage and capacity	Driving range
Honda FCX-V3	Compact Car	2000	60	100 L at 250 atm	180 km
Honda FCX-V4	Compact Car	2002	60	137 L at 350 atm	315 km
Honda FCX 2nd Generation	Compact Car	2004	80	156.6 L at 350 atm	430 km
Honda FCX Clarity FCEV	Compact Car	2007	100	3.92 kg at 5000 psi	240 miles
Chevrolet HydroGen3	Minivan	2001	60	3.1 kg at 700 bar/4.6 kg at -253 °C	270 km/400 km
Chevrolet Sequel	Cross-over SUV	2005	73	8 kg at 700 bar	300 miles
Chevrolet Equinox FCV	Sport utility vehicle	2008	93	4.2 kg at 700 bar	200 miles
Toyota FCHV	Sport utility vehicle	2001	90	350 bar	180 miles
Toyota FCHV	Sport utility vehicle	2005	90	350 bar	200 miles
Toyota FCHV-adv	Sport utility vehicle	2009	90	156 L at 700 bar	430 miles
Kia Borrego	Sport utility vehicle	2009	109	-	426 miles
Daimler B-Class	Compact car	2009	100	700 bar	400 km
Passat LingYu	Sedan	2008	55	-	186 miles

2.1.2 Buses

Fig. 4 shows the number of fuel-cell buses commercialized each year from 1994 through 2008. Several government-funded procurement plans were announced recently, such as the US National Fuel Cell Bus Program and Europe’s Fuel Cell and Hydrogen Joint Technology Initiative. The number is expected to increase in the near future.

Due to the CUTE and similar programs, over half of the commercialized fuel-cell buses are running in Europe, a quarter in Asia, and 15% in North America. In North America, California is the main region of fuel cell bus activity, primarily due to the ZEV regulation approved by the California Air Resources Board (CARB) [14].

2.1.3 Other vehicles or propulsions

In addition to buses and light-weight automobiles, PEM fuel cells may be employed in several other applications within the transportation/propulsion sector. These applications include electric powered bicycles, material handling vehicles such as forklifts, and auxiliary power units (APUs) including leisure, trucking, marine and Unmanned Aerial Vehicles (UAVs) [15]. Hwang et al. [16] developed an electric bicycle powered by a 40-cell stack, which exhibits a peak power of 378 W, a maximum speed of 16.8 km/h and an efficiency of up to 35%.

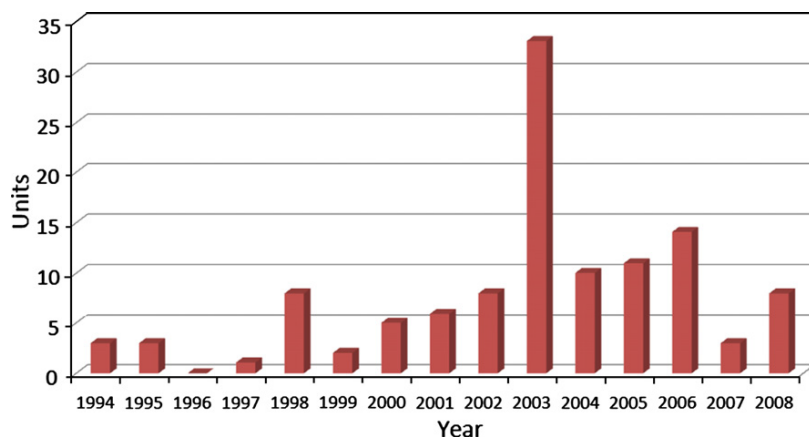


Fig.4 Fuel-cell buses commercialized each year from 1994 through 2008

Table 2 lists major companies in this fuel cell transportation sector. In addition, fuel cell applications in the transportation sector require onboard hydrogen storage tanks and their success also rely on the presence of hydrogen fuelling infrastructure. In the latter regard, governments play a decisive role in the development of hydrogen fuelling network.

Table 2

A list of key companies in the fuel cell transportation sector

Company	Website	Location	Details
BAE Systems	baesystems.com	UK	Integration of a fuel cell APU into its hybrid bus powertrain
Ballard	ballard.com	Canada	FC forklifts; HD6, their next generation engine for hybrid fuel-cell buses
Daimler	daimler.com	UK	Fuel-cell buses, the new BlueZERO FCV
General Motors	gm.com	USA	115 units of its fourth generation Equinox FCV, which have been delivered to California, Germany, China, Korea and Japan
H2Logic	h2logic.com	Denmark	FC forklifts, focusing on the European market
Honda	honda.com	Japan	200 of its FCX clarity are expected to be shipped to California and to government members in Japan within the next 3 years, FC sport, which uses the FCX clarity technology in a sport-like designed car
Hydrogenics	hydrogenics.com	Canada	20 kW minibuses, APUs and range extenders
Hyundai-Kia	worldwide.hyundai.com	Korea	Borrego FCEV, using four generation FC technology and is expected to have a 426-mile range
Nissan	nissan-global.com	Japan	X-TRAIN SUV, equipped with Nissan's latest generation FC system, provided Renault with FC technology for Renault's hybrid drive FC Scenic
Nuvera	nuvera.com	USA	PowerEdge, hybrid FC forklifts, 82 kW FC bus
Oorja Protonics	oorjaprotonics.com	USA	DMFC-based charger for forklifts' batteries
Proton Motor	proton-motor.de	Germany	Zemship FC passenger ferry, FC powered street sweeper, light duty truck
Protonex	PROTONEX.com	USA	APUs, UAVs (Unmanned Aerial Vehicles)
Toyota	toyota.com	Japan	40 units of its latest FCHV-adv unveiled in Japan
Tropical S.A.	tropical.gr	Greece	Hybrid FC bikes and scooters, with the FC charging the battery
UTC power	utcpower.com	USA	120 kW PureMotion system for FC buses, and 120 kW FC cars
Volkswagen	volkswagen.com	Germany	16 units of its Passat Lingyu shipped to California for demonstration and testing
Volvo	volvo.com	Sweden	APUs

2.2 Portable applications

The fast-growing power demand by portable electronic devices is unlikely satisfied by current battery technology because of its low energy power capability and long charging time. These two issues can be well resolved by using portable/micro PEM fuel cells. Consequently, global production of portable fuel cells has continuously grown, as shown in Fig. 5.

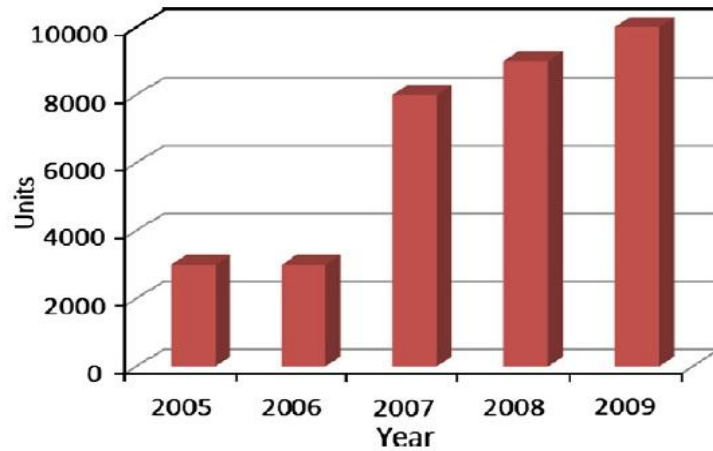


Fig. 5 Portable PEMFC units commercialized.

Over two-thirds of these units are based on regular PEM fuel cells, a quarter of them consist of DMFC (direct methanol fuel cell) units and the remaining 6% are not related to PEM technology [17]. The typical power range for portable electronic devices is 5–50W and several developments focus on a level of <5W for micro power application [12]. A wider range of power, 100–500 W, has also been considered [18]. Many approaches have been proposed for portable/micro fuel cell fabrication. Hayase et al. developed a technique to pattern fuel cell channels and GDL (gas diffusion layer) in Si wafers [19]. Lee et al. employed LIGA (which refers to the German acronym for X-ray lithography-technique: X-ray Lithographie, Galvanoformung (electrodeposition), and Abformtechnik (molding)) to fabricate flow channels in metallic bipolar plates [20]. Ito et al. utilized a technique similar to that used for machining of compact disks to create micro grooves in metal plates [21]. Hahn et al. used reactive ion etching (RIE) to machine microchannels in stainless steel plates [22]. Hsieh et al. proposed a SU-8 photoresist microfabrication process for the fuel cell flow structures [23]. Cha et al. employed various micro/nanofabrication processes, such as lithography, physical vapor deposition (PVD), and focused ion beam (FIB) etch/deposition, to fabricate flow field plates [24]. Madou and co-workers used carbon obtained by pyrolyzing polymer precursors (called the “C-MEMS process) for the bipolar fluidic plates [25-27]. Fig. 6 shows the bipolar plates with a serpentine flow field after and before carbonization using C-MEMS.

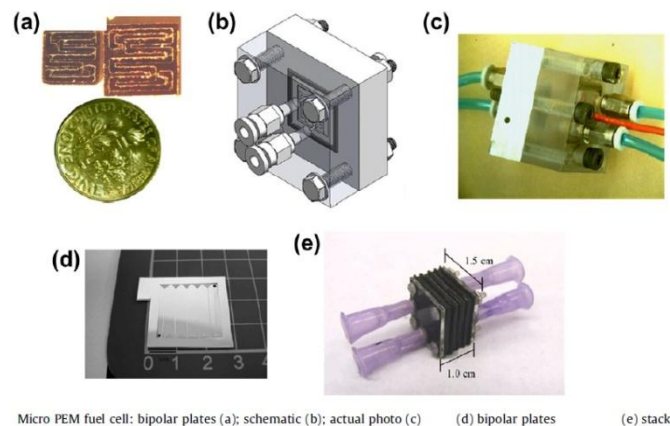


Fig.6

The micro channels are in serpentine pattern with a cross-section of 0.8 mm. Fig. 6 also shows the assembled micro PEM fuel cell (0.8 x 0.4 cm), fuel cell bipolar plates and stack. Henriques et al. [28] discussed the efficiency improvement by altering the cathode channel geometry and achieved an efficiency increase up to 26.4%. In addition to mobile phones and laptops, portable fuel cells can be used to power toys and utilities such as RC (radio control) cars, boats, robot toys, and emergency lights (e.g. for mining). Fig. 10 displays the hobby-

grade vehicles based on Horizon’s H-Cell fuel cell system (specifics are listed in Table 4). Fuel cell also receives a great deal of attentions for military application to power portable electrical devices such as radios. Table 3 lists several major companies in the portable PEMFC sector.

Table 3

Major companies in the portable PEMFC sector			
Company name	Website	Location	Details
CMR fuel cells	cmrfuelcells.com	UK	25 W hybrid DMFC laptop battery charger
Viaspace/direct methanol fuel cell corporation	viaspace.com/ae_dmfcc.php	USA	Disposable fuel cartridges for DMFCs
Jadoo power systems	adoopower.com	USA	Chemical hydride fuels for fuel cells, 100 W portable electric power supply for aeromedical evacuation applications
Horizon	horizonfuelcell.com	China	H-racer series of toys and gadgets, hobbyist fuel cell systems
MTI micro	Timicrofuelcells.com	USA	Collaboration with equipment manufacturers about external chargers, including universal chargers
Neah power systems	neahpower.com	USA	DMFC units
Samsung DSI	samsungdsi.com	Korea	Military DMFC battery with up to 800% more durability and 54% more power
SFC Smart Fuel Cell	sfc.com	Germany	APUs for camping and leisure, a portable soldier-worn military fuel cell system
Sony	sony.co.jp	Japan	DMFC powered recharging devices for laptops and mobile phones
Toshiba	toshiba.co.jp	Japan	10 W DMFC battery charger

1.3. Stationary applications

Current stationary electric power is primarily generated by large central power stations. Large-scale central power stations have many benefits such as high efficiency, but exhibit several inherent disadvantages, e.g. the waste heat that usually cannot be efficiently utilized (due to the costly long-distance transport) and power loss during transmission. Distributed power decentralized generation is a way to resolve these disadvantages, which cogenerates heat and power for local usage, a diagram of which can be seen in Fig. 7.

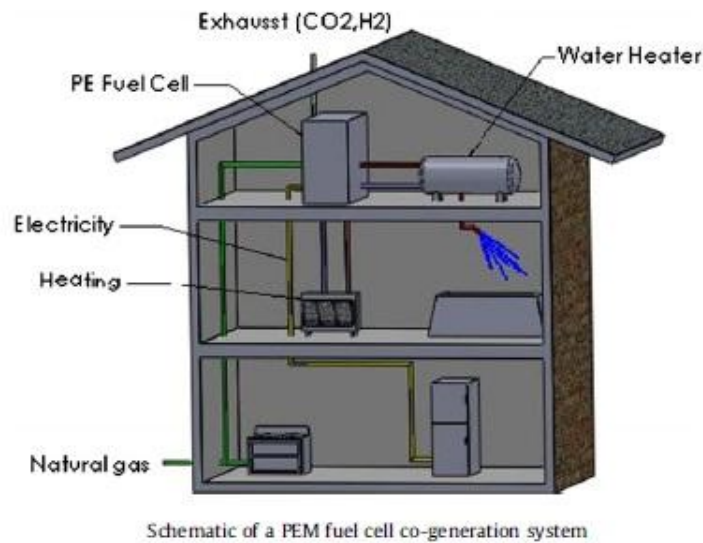


Fig. 7.

Both ICEs and fuel cells can be applied for decentralized small-scale stationary power generation. Except cost, fuel cells exhibit several important advantages over ICEs, such as high electric power conversion efficiency, low noise, zero emission, and easy scale-up. In this sector, distributed PEM fuel cell systems can be employed to several areas such as heat-power co-generation for household/residential use and uninterruptable power supply (UPS). The former requires further significant improvement in fuel cell cost and lifetime. However, currently few fuel cell units have exhibited a lifetime over 10,000 h. Several units are now available in the market: the GenSys™ Blue CHP (combined heat and power) system by Plug Power was developed to be compatible with existing home heating systems such as forced air or hot water; the FCgen™- 1030V3 stacks developed by Ballard Power Systems can be incorporated into the residential CHP systems in the market. The latter area such as back-up, remote, and uninterrupted power received a growing attention in recent years. The

back-up power market is particularly promising for potential customers such as banks, hospitals, and telecom companies which require reliable powers to maintain their business/operation and avoid unexpected power breakdowns. The GenSys™ fuel cell system has been developed for this application and delivered to more than 50 customer locations in more than 10 countries based on the 2005's data. In 2009 Plug Power received a \$1.4 million award from the New York State Energy Research and Development Authority (NYSERDA) to install and operate three CHP GenSys™ fuel cell systems in New York State homes [29]. Plug Power also expects to install approximately 1000 systems throughout India by the end of 2010 [30]. FCgen™ units of Ballard Power Systems have been supplied to IdaTch LLC for use by ACME Group at telecom cellular tower sites in India; and Ballard also works with Dantherm Power A/S of Denmark to provide back-up power solutions to telecommunications providers [31].

Table 4

Several major fuel cell companies in the small stationary sector			
Company	Website	Location	Details
Altergy	www.altergy.com	USA	Fuel cell stacks and systems for the UPS market
ClearEdge	www.dearedgepower.com	USA	5 kW CES natural gas fuelled CHP unit
Ebara Ballard		Japan	JV between Ballard and Ebara, 1 kWe PEM system
Eneos Celltech		Japan	JV between Sanyo Electric and Nippon Oil, PEM and SOFC residential units
Hydrogenics	www.hydrogenics.com	USA	HyPM-XR, for integration in UPS datacenter cabinets and HyUPS for mobile phone
IdaTech	www.idatech.com	USA	Has deal to supply up to 30,000 5 kW UPS systems to the Indian ACME group.
Matsushita		Japan	Delivered 650-1 kWe stacks
P21	www.p-21.de	Germany	Spin out from Vodaphone, now supplies PEM UPS systems
Plug Power	www.plugpower.com	USA	GenSys low temperature units is being marketed to telecommunication sector
Toshiba FCP		Japan	1 kW, wants to be shipping 40,000 units per annum in Japan by 2015

2.4 Needs on fundamental research

Phenomena involved in PEM fuel cell operation are complex; specifically, they involve heat transfer, species and charge transport, multi-phase flows, and electrochemical reactions. Fundamentals of these multi-physics phenomena during fuel cell operation and their relevance to material properties are critically important to overcome the two major barriers, namely durability and cost. These phenomena occur in various components, namely the membrane electrode assembly (MEA) consisting of the catalyst layers (CL) and membrane, gas diffusion layer (GDL) and micro-porous layer (MPL) (together referred to as diffusion media (DM)), gas flow channels (GFCs), and bipolar plates (BP). The cost ratio of the major components is shown in Fig. 2.

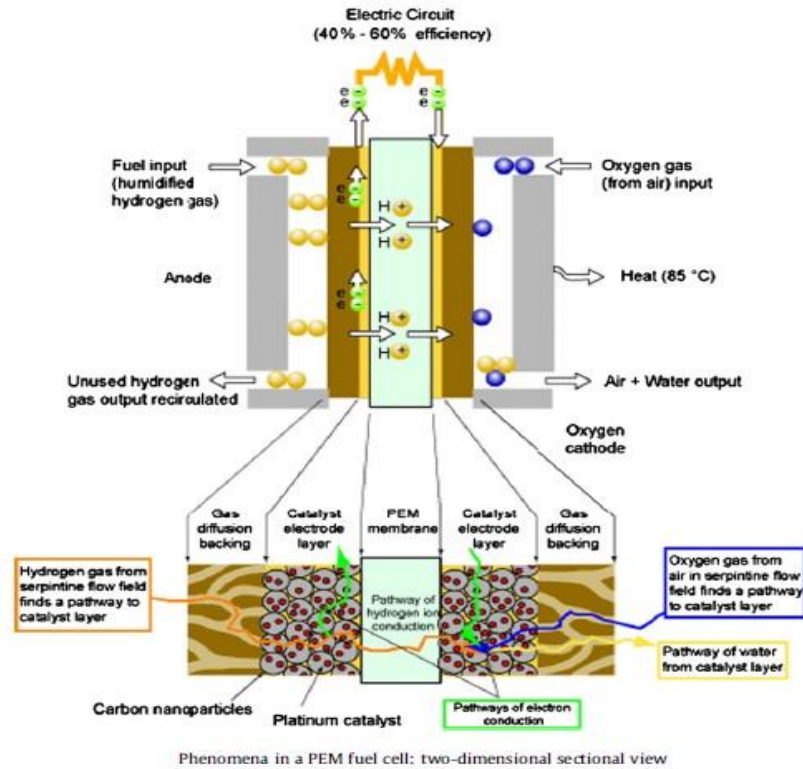


Fig. 8

Specifically, as schematically shown in Fig.8, the following multi-physics, highly coupled and nonlinear transport and electrochemical phenomena take place during fuel cell operation: (1) hydrogen gas and air are forced (by pumping) to flow down the anode and cathode GFCs, respectively; (2) H₂ and O₂ flow through the respective porous GDLs/MPLs and diffuse into the respective CLs; (3) H₂ is oxidized at the anode CL, forming protons and electrons; (4) protons migrate and water is transported through the membrane; (5) electrons are conducted via carbon support to the anode current collector, and then to the cathode current collector via an external circuit; (6) O₂ is reduced with protons and electrons at the cathode CL to form water; (7) product water is transported out of the cathode CL, through cathode GDL/MPL, and eventually out of the cathode GFC; and (8) heat is generated due to inefficiencies, mainly in the cathode CL due to the sluggish oxygen reduction reaction (ORR), and is conducted out of the cell via carbon support and BPs. The transport phenomena are three-dimensional because the flows of fuel (H₂) and oxidant (O₂) in the anode and cathode GFCs are usually normal to proton transport through the membrane and gas transport through the respective GDLs/MPLs and CLs. When operating under practical current loads, relatively high inlet humidity, liquid water is present within the fuel cell. Fundamental models have been developed to examine the transport processes; Tables 5 and 6 list a set of governing equations, based on the laws of conservation of mass, momentum, energy, species and charges and the multi-phase mixture formulation [32-36].

Table 5

Fuel cell governing equations		
Continuity equation	$\epsilon \frac{\partial \rho}{\partial t} + \nabla \cdot (\rho \vec{u}) = S_m$	(1)
Momentum conservation	$\frac{1}{2} \left[\frac{\partial \vec{u}}{\partial t} + \frac{1}{2} \nabla \cdot (\vec{u} \vec{u}) \right] = -\nabla (\frac{p}{\rho}) + \nabla \cdot \tau + S_u$	(2)
Energy conservation	$\frac{\partial \rho c_p T}{\partial t} + \nabla \cdot (\gamma_T \rho c_p \vec{u} T) = \nabla \cdot (k^{eff} \nabla T) + S_T$	(3)
Species conservation (H ₂ O/H ₂ /O ₂)	$\epsilon^{eff} \frac{\partial c^k}{\partial t} + \nabla \cdot (\gamma_c \vec{u} c^k) = \nabla \cdot (D^{k,eff} \nabla c^k) - \nabla \cdot \left[\left(\frac{m_i^k}{M^k} - \frac{c_i}{\rho} \right) \vec{j}_i \right] + S_k$	(4)
Charge conservation (electrons)	$0 = \nabla \cdot (\sigma^{eff} \nabla \Phi_s) - S_\phi$	(5)
Charge conservation (protons)	$0 = \nabla \cdot (\kappa^{eff} \nabla \Phi_e) + S_\phi$	(6)

Table 6

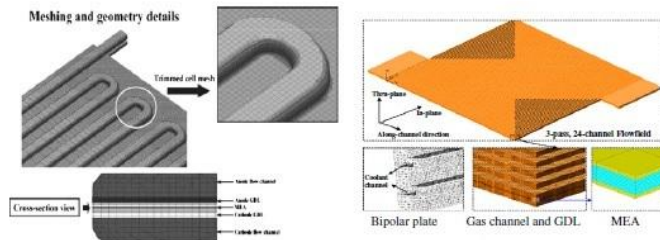
Source terms for the conservation equations in each region					
	S_m	S_u	S_k	S_p	S_T
GFC	0	0	0	-	S_R
DM	0	$-\frac{\mu}{n_d a} \vec{u}$	0	0	$\frac{\rho \vec{u}^2}{2} + S_R$
Catalyst Layer	$M^w \nabla \cdot (D_m^w \nabla C^w) + \sum_k S_k M^k$	$-\frac{\mu}{n_d a} \vec{u}$	$-\nabla \cdot (\frac{n_d}{F} i_k) - \frac{S_d}{n_d F}$	j	$j \left(\eta + T \frac{d\eta}{dT} \right) + \frac{\rho \vec{u}^2}{2} + \frac{\rho \vec{u}^2}{2} + S_R$
Membrane	0	-	0	0	$\frac{\rho \vec{u}^2}{2}$

Electrochemical reaction
 $\sum_k S_k M_k = n e^-$
 In PEM fuel cells, there are:
 (Anode) $H_2 - 2H^+ = 2e^-$
 (Cathode) $2H_2O - O_2 - 4H^+ = 4e^-$

where $\begin{cases} M_k \equiv \text{chemical formula of species } k \\ S_k \equiv \text{stoichiometry coefficient} \\ n \equiv \text{number of electrons transferred} \end{cases}$

Note: n_d is the electro-osmotic drag coefficient for water. For H_2 and O_2 , $n_d = 0$.

Table7 lists the typical ranges of the mostmodel parameters. Figs.9 and 10 show examples of computational meshes used in large-scale simulation of a single PEM fuel cell with the major components and predicted current density distribution in the membrane, respectively. A large variation of reaction current density is indicated in the figure, and this detail information will aid the design and fundamental study of PEM fuel cell, in particular helping PEMFC developers overcome the two major barriers. The remaining of this session details what fundamentals are considered understood, what are partially understood, what are not yet understood but need further study.



Computational mesh at bending channel location of 480 cm² reaction area (~5 million gridpoints) (left) [273]; and computational domain of a 200 cm² PEFC (right) (~23 million gridpoints)

Fig.9 Computational meshing

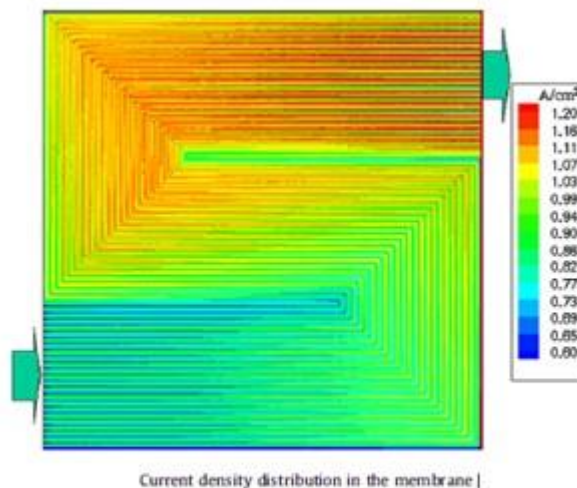


Fig. 10 Current density distribution in membrane.

Table 7

The electrochemical and transport properties that are frequently used		
Description	Unit	Value
<i>Electrochemical kinetics</i>		
Exchange current density (Anode, Cathode), i_0	A/m ²	10 ³ , 10 ³ -10 ⁴
Faraday constant, F	C/mol	96487
Electrical conductivity of DMs, BPs, σ^{eff}	S/m	300, 20000
<i>Species transport properties</i>		
H ₂ /H ₂ O diffusivity (H ₂ -H ₂ O) at standard condition, D^k	m ² /s	8.67/8.67 × 10 ⁻⁵
O ₂ /H ₂ O (v) diffusivity in the air at standard condition, D^k	m ² /s	1.53/1.79 × 10 ⁻⁵
Viscosity at 80 °C (H ₂ /Air), D^k	m ² /s	9.88 × 10 ⁻⁶ /1.36 × 10 ⁻⁵
<i>Thermal properties</i>		
H ₂ /N ₂ /O ₂ /H ₂ O(v) thermal conductivity, k^{eff}	W/m K	0.170/0.024/0.024/0.024
Anode/cathode GDL conductivity, k^{eff}	W/m K	0.3-3
Anode/cathode CL conductivity, k^{eff}	W/m K	0.3-1.5
Membrane thermal conductivity, k^{eff}	W/m K	0.95
Anode/cathode bipolar plate thermal conductivity, k^{eff}	W/m K	>10.0
H ₂ /N ₂ /O ₂ /H ₂ O(v) specific heat at 80 °C, c_p	J/kg K	14400/1041/917/2000
Anode/cathode GDL heat capacity, ρc_p	J/K m ³	5.68 × 10 ⁵
Anode/cathode CL heat capacity, ρc_p	J/K m ³	1.69 × 10 ⁶
Membrane heat capacity, ρc_p	J/K m ³	1.65 × 10 ⁶
Anode/cathode bipolar plate heat capacity, ρc_p	J/K m ³	1.57 × 10 ⁶
Latent heat of liquid water-vapor/liquid-solid water phase change	J/kg	2.26 × 10 ⁶ /3.34 × 10 ⁵
<i>Material properties</i>		
Permeability of anode/cathode GDL, $K_{C,DL}$	m ²	1.0 × 10 ⁻¹²
Permeability of anode/cathode CL, K_{CL}	m ²	1.0 × 10 ⁻¹³
Anode/cathode GDL porosity, ϵ		0.4-0.8
Anode/cathode CL porosity, ϵ		0.3-0.5
Ionomer volume fraction in CL, ϵ_{ion}		0.13-0.4
Equivalent weight of ionomers, EW	kg/mol	0.9, 1.1 or 1.2*
Dry density of membrane, ρ	kg/m ³	1.98 × 10 ³

*Several typical Nafion® membranes.

III. Membrane electrode assembly

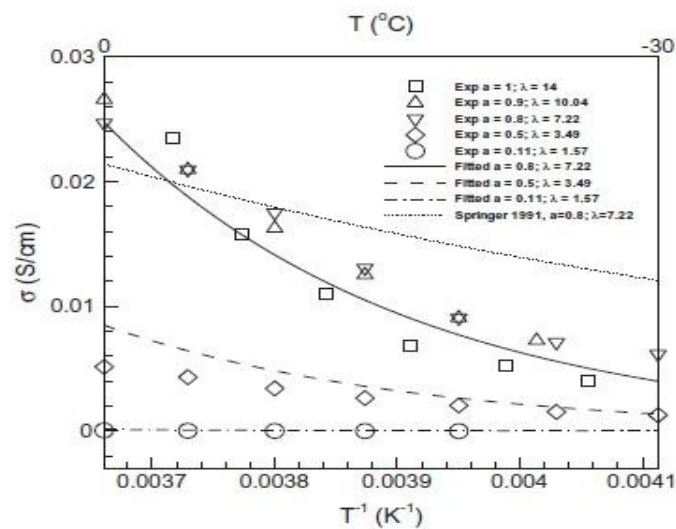
3.1. MEMBRANE

Membrane refers to a thin layer of electrolyte (usually 10– 100 μm , e.g. 18 μm for Gore 18 and 175 μm for Nafion, which conducts protons from the anode to the cathode. Desirable membrane materials are those that exhibit high ionic conductivity, while preventing electron transport and the cross-over of hydrogen fuel from the anode and oxygen reactant from the cathode. In addition, they must be chemically stable in an environment with HO– and HOO radicals, thermally stable throughout the operating temperatures, and mechanically robust. Current membranes are mostly based on the perfluorosulfonic acid, the most prominent of which, Nafion, was first developed by the DuPont Company in 1960s. Nafion has a backbone structure of polytetrafluoroethylene (PTFE, known by the trade name Teflon), which provides membrane with physical strength. The sulfonic acid functional groups in Nafion provide charge sites for proton transport. Additionally, other perfluorinated polymer materials such as Neosepta-F™ (Tokuyama), Gore-Select™ (W.L. Gore and Associates, Inc.), Flemion™ (Asahi Glass Company), Asiplex™ (Asahi Chemical Industry) are also adopted for PEM fuel cell applications. In addition, membrane materials that can operate at high temperatures (100-200°C) are preferred for high temperature PEM fuel cell which has advantages of better catalyst tolerance to CO and cooling strategy for fuel cell [37,38]. The Nafion-based membranes are costly primarily due to their complex fabrication process [39]. Research on cost-effective high-performance electrolyte materials has been active in the entire course of fuel cell development. Solvay Solexis is developing Hyflon ionomers, also known as short side chain (SSC) ionomer (which was originally developed by Dow Chemicals Company and then abandoned [40]) that can exhibit a better performance and durability than Nafion in several cases. However, severe degradation has been observed for this membrane material [41]. Phosphoric acid-doped polybenzimidazole (PBI) membrane is a promising material for high temperature membrane due to its high proton conductivity at temperatures up to 200 C and low methanol/ ethanol permeability. However, there are concerns on low proton conductivity at low temperature (important for cold start) and low solubility of oxygen along with evaluation of stack components including bipolar plates, seals and coolant, and thermal and water management [42]. Hydrocarbon-based membranes have been attempted by PolyFuel for fuel cell [43]. Two major transports take place in membranes, i.e. proton and water transport. Gierke and Hsu described the polymeric membrane, known as a cluster model, in terms of an inverted micellar structure in which the ion-exchange sites are separated from the fluorocarbon backbone, forming spherical clusters (pores), connected by short narrow channels [44]. The cluster sizes depend on local water content. The main driving force for proton transport is the gradient of electrical potential of the electrolyte. That is, protons transport across the membrane mainly due to the existence of electrolyte potential gradient; the effect of diffusion is relatively small. Water in the membrane is essential for proton transport: one mechanism is called the “vehicular” diffusion. By forming hydronium ions (H₃O⁺), protons, can transport from high to low proton concentration regions, which is called the vehicular diffusion [45]. Therefore, this mechanism largely depends on the diffusivity of water in membranes. Another is through the “Hopping”

mechanism that takes place when sufficient water content is presented so that the side chains of sulfonic groups are connected, where protons can move directly from one site to another [46,47]. One of the most prevalently used proton-conductivity models is the empirical correlation developed by Springer et al. [48] for the Nafion 117 membrane, as follows

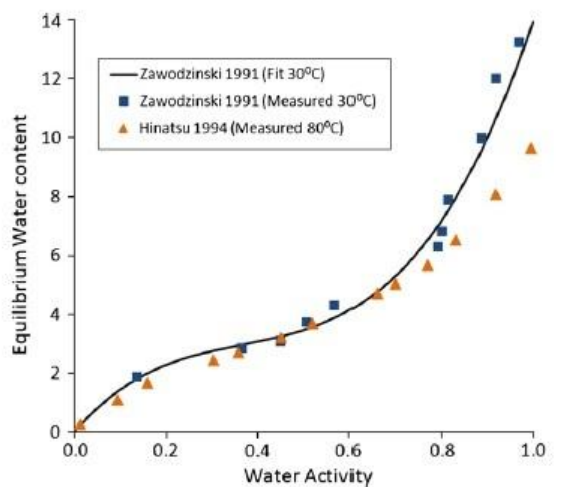
$$\kappa = (0.005193\lambda - 0.00326) \exp \left[1268 \left(\frac{1}{303} - \frac{1}{273 + T_{\text{cell}}} \right) \right] \dots\dots\dots(7)$$

At subfreezing temperature, the Nafion membrane remains conductive to protons due to the existence of non-frozen water in the membrane, see Fig. 11 [49-52]. The water content λ , usually defined as the number of moles of water per mole of acid sites attached to the membrane (namely, SO₃H), is related to the water activity of the surrounding fluids, see Fig. 12



Ionic conductivity of the membrane at subfreezing conditions

Fig.11



Equilibrium water uptake relation for Nafion® membranes at 30 °C

Fig. 12

Though current correlations are mostly simple and easy to implement in a full fuel-cell computer model but only valid for the conditions under which the fitted data was collected. For each new membrane, a whole new set of data must be generated at the conditions of interest. Therefore, a better model of proton conductivity is highly needed [53]. Another important membrane property is the water diffusivity which also depends on the local membrane water content, see Fig. 13 [48,53]. In addition to diffusion, the electro-osmotic drag (EOD) can transport water from the anode to cathode and the EOD coefficient might be a function of water content (both linear and stepwise correlations have been proposed.) [54-59].

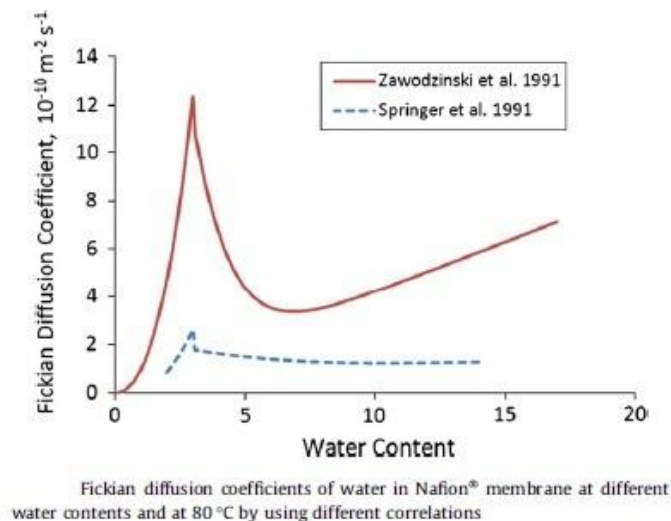


Fig. 13

When liquid water is present at the membrane surfaces, hydraulic permeation can take place [60], which is driven by the pressure difference at the membrane surfaces. A correlation, proportional to the membrane water content, was proposed by Bernardi and Vergrugge [61] and Büchi and Srinivasan [62]. Ionic and water transport in membranes plays an important role in fuel cell operation. The ionic transport resistance directly determines the Ohmic loss of cell voltage and associated Joules heating. Formation of local hot spots may occur at high resistance sites, leading to membrane pin-hole formation and other degradation issues. A sufficient hydration level of membranes is critical to their ionic conductivity. It has also been observed that dryness of membranes may cause cracks and degradation issues. In addition, using experimental data obtained by Zawodzinski et al. [55,63], Springer et al. [48] developed an empirical correlation relating proton conductivity to water content in the membrane, see Eq. (7). They also correlated the electro-osmotic drag coefficient with water content. These two empirical correlations put forth by Springer et al. enjoy widespread usage in the PEMFC literature. Recently, Chen and Hickner [64,65] formulated a new constitutive model for predicting proton conductivity in polymer electrolyte. Their conductivity model depends on the molar volumes of dry membrane and water but otherwise requires no adjustable parameter. Predictions computed from Chen and Hickner's conductivity model yield good agreement with experimental data from the literature and those from their own measurements for a wide range of water contents. Weber and Newman [66,67] developed a comprehensive membrane model that treats membrane swelling and seamlessly and rigorously accounts for both vapor and liquid- equilibrated transport modes using a single driving force of chemical potential. The transition between the two modes is determined based on the energy needed to swell and connect the waterfilled nano-domains. However, there are still some discrepancies to be overcome such as an underestimation of the interfacial water mass-transport resistance and a lack of consideration of membrane state or history.

3.2. Catalyst layers

The catalyst layer (CL) is where the hydrogen oxidation reaction (HOR) or oxygen reduction reaction (ORR) takes place. CL is usually very thin (about 10 μm). Several phases contained in a CL are key to the electrochemical reaction: (1) carbon support with Pt catalyst particles dispersed on the carbon surface, (2) ionomer, and (3) void space. The catalyst plays the critical role of reducing the reaction activation barrier. Hydrogen fuel is oxidized in the anode whereas the ORR takes place in the cathode (see Table 6). Platinum or

platinum alloy is popular catalyst for both the ORR and HOR, therefore the CL contributes a significant portion of cost for a fuel cell. Pt and several of its alloys (Pt–Co, Pt–Ni, Pt–Fe, Pt–V, Pt–Mn and Pt–Cr) exhibit good catalyst kinetics [68,69,70,109,114,117]. The Pt loading is an important factor in the CL development. The DOE target is 0.3 and 0.2 mg/cm² for 2010 and 2015, respectively, and most recently the 3 M Company achieves 0.15 mg/cm² with PtCoMn alloy [71]. In addition to Pt-loading reduction, one active research area is to explore new catalyst materials. Two major approaches have gained momentum. The first of which is to replace the Pt with another less expensive precious metal, such as ruthenium or palladium [72,73]. The second is to use non-precious metal catalysts (NPMC). Bashyam and Zelenay examined the cobalt–polypyrrole– carbon (Co–PPY–C) composite. This catalyst exhibits good activity with a Co loading of 6.0X 10⁻² mg cm⁻² and stability in PEM fuel cells, and generates 0.2A/cm² at 0.50 V and a peak power density of 0.14 W/cm² [74]. Some studies are focused on heat-treated Fe and Co–N/C catalysts, of which a review is given by Bezerra et al. [123]. A review on materials such as Cu, Pd/Co, Mo₄.2Ru1.8Se₈, WC + Ta and LaMnO₃+o was provided by Wang [124]. Most recently, a comprehensive work on NPMCs was presented by Zelenay [75]. They achieved an OCV of 1.04 V and volumetric ORR activity of 165 A/cm³ (volume based on electrode and over 100 times improvement) with Cyanamide– Fe–C catalyst, which meets the DOE 2010 target. In addition, CO adsorption at the Pt site causes severe loss in performance. To improve the CO tolerance by PEM fuel cells, the use of binary Pt–Ru catalysts and oxygen bleeding technique were proposed in 1980s and 1990s [76,77] and various materials for CO tolerant catalysts (Zeolite support, Pt–Mo, Sulfided catalysts, etc) are under research [78]. Improving the Pt utilization is another way for reducing the Pt loading and CL cost. The reactions take place at the triple-phase boundaries; the area of this active catalyst surface is usually large to improve the Pt utilization. This can be directly seen from the well-known Butler–Volmer equation:

$$\sigma \cos(\theta_{c,GDL}) \left(\frac{\varepsilon_{GDL}}{K_{GDL}} \right)^{1/2} J(s) = P_{c,GDL} = P_{c,MPL}$$

$$= \sigma \cos(\theta_{c,MPL}) \left(\frac{\varepsilon_{MPL}}{K_{MPL}} \right)^{1/2} J(s)$$

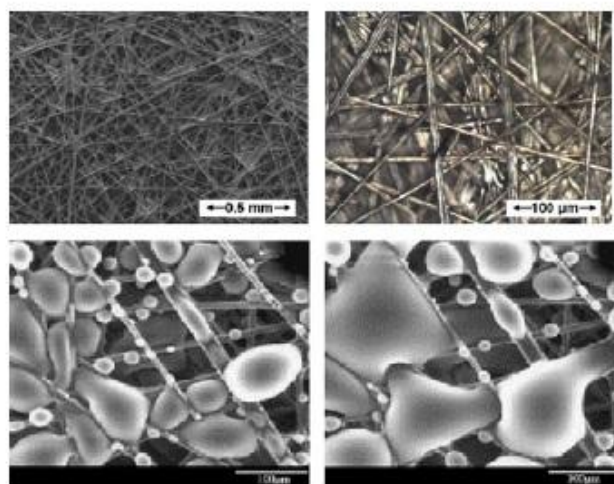
.....(8)

where *j* is the reaction current or transfer current per unit volume, *i*₀ the exchange current density, *a* the specific active area per unit volume, *F* the faraday constant, *R* the universal gas constant, and *g* the surface overpotential. The value of *a* is usually 100–1000, significantly increasing the catalytic activity, which is related to the structural information of CLs.

In addition, avoiding CL flooding is of critical importance for optimal PEMFC performance and durability; however it is not well understood. The ability to model transport and electrochemical reactions in CLs is crucial, particularly for the cathode in which the ORR is sluggish and inefficient and water is generated. The water content of the cathode CL directly affects the protonic conductivity in this domain and thus the reaction-rate distribution. There is a great need to elucidate mechanisms of liquid-water transport/evaporation in the CL and the interactions with the CL microstructure and wettability and to develop a predictive tool to enable microstructural and surface prototyping of future generations of CL. Some CL component models have been developed by Siegel [79] and Siegel et al. [80], Harvey [81], Harvey et al. [82], Marr and Li [83], Schwarz and Djilali [84], and Shah et al. [85], but they need to be improved and integrated into the full PEMFC model. Specially, Harvey et al. [82] compared three different approaches for describing the cathode catalyst layer: namely, a thin-film model, discrete-catalyst volume model, and agglomerate model. They indicated that for a given electrode overpotential, the thin-film model significantly over-predicts the current density and exaggerates the variation in current density both along and across the channel, and the agglomerate model predicts noticeable mass transport losses. In addition, the CL is usually thin, but may be subjected to mass transport limitation or a considerable ohmic loss. In this regard, further reducing the CL thickness is necessary to improve its performance. A CL model that properly captures the key transport phenomena and the HOR or ORR reaction at the three-phase interface can be employed to optimize the CL thickness. Specifically, such a model can elucidate the effect of catalyst-layer thinning on PEMFC performance. Furthermore, thinner CLs (in the scale of 1 μm) can reduce the catalyst loading and hence the CL cost. Research efforts are definitely needed in this area.

3.3. Gas diffusion layers and micro-porous layers

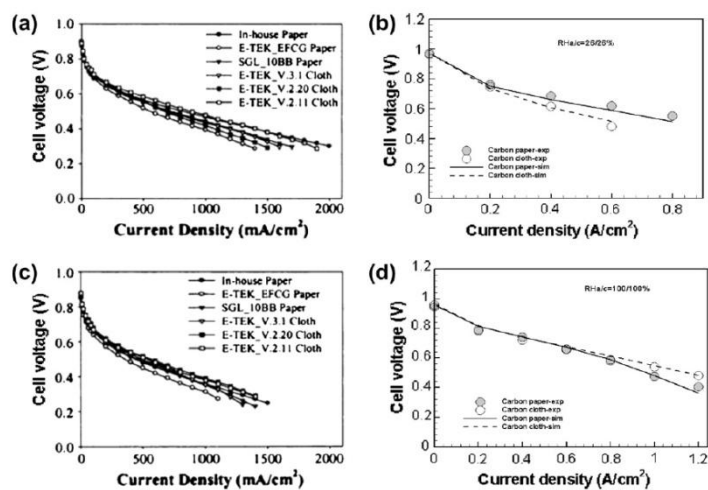
Gas diffusion layers (GDLs) and micro-porous layer (MPLs), together called DM (diffusion media), play multiple roles: (1) electronic connection between the bipolar plate with channel-land structure and the electrode, (2) passage for reactant transport and heat/water removal, (3) mechanical support to the membrane electrode assembly (MEA), and (4) protection of the catalyst layer from corrosion or erosion caused by flows or other factors [86,87]. Physical processes in GDLs, in addition to diffusive transport, include bypass flow induced by in-plane pressure difference between neighboring channels [88,89], through-plane flow induced by mass source/sink due to electrochemical reactions [90,91], heat transfer [92,93] like the heat pipe effect [94], two-phase flow [94,95], and electron transport [61,96]. Transport inside GDLs, closely related to the GDL structural feature, plays an important role in fuel cell energy conversion. GDLs are usually 100–300 μm thick. A popular GDL material is the carbon fiber based porous media: the fibers are either woven together to form a cloth, or bonded together by resins to form a paper, see Fig. 14.



The carbon paper DM (above) and two consecutive environmental scanning electron micrographs (ESEM) of a diffusion medium exposed to water-vapor saturated atmosphere (below)

Fig. 14.

Wang et al. further presented detailed DNS to disclose the transport phenomena of mass, reactant, electron, and heat occurring inside the GDL, see Figs. 15 and 16 [97].



Cell performance using different DMs at: the 80 °C/75% RH cathode inlet condition (a), the 100 °C/70% RH cathode inlet condition and 80 °C (c); and 100/100% RH and 80 °C (d). (b): 25/25% RH for anode/

Fig 15 Cell performance for variable conditions

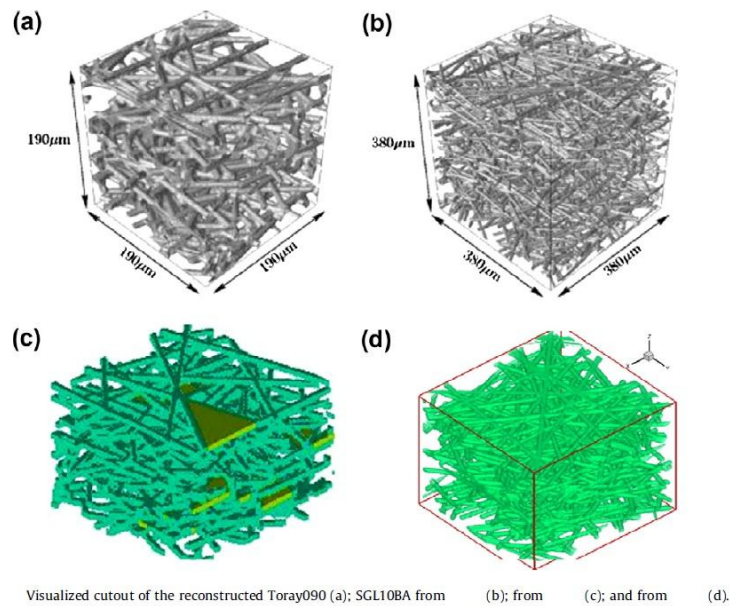
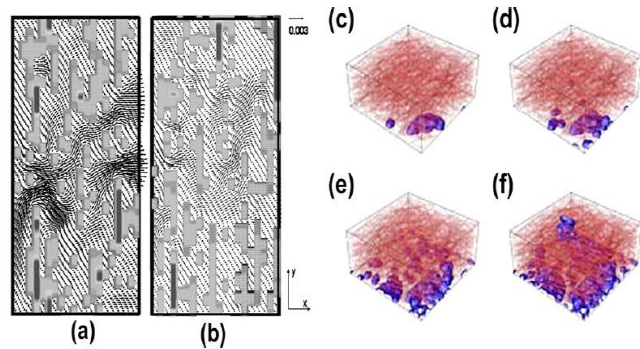


Fig.16

Wang and co-workers [98-100] applied the LBM (Lattice Boltzmann method) to study the meso-scale transport of liquid water, based on detailed GDL structure either from stochastic modeling or experimental imaging (e.g. X-ray micro-CT). The LBM is a powerful technique for simulating transport and fluid flows involving interfacial dynamics and complex geometries. It is based on first principles and considers flows to be composed of a collection of pseudo-particles residing on the nodes of an underlying lattice structure. The LBM formula is different from the conventional Navier–Stokes equation, which is based on macroscopic continuum description. Comparing with VOF (volume of fluid) methods, the LBM is advantageous in simulating multi-phase flows because of its inherent ability to incorporate particle interactions to yield phase segregation and thus, eliminate explicit interface tracking. An example of prediction using the LBM is shown in Fig. 17. Using 3D tomography image, Becker et al. [101,102] applied a simplified model to determine permeability, diffusivity, and thermal conductivity as a function of liquid saturation.

Multi-phase flow, originated from the water production by the ORR, is critical to fuel cell water management. The excessive presence of liquid water hinders the reactant delivery to the catalyst sites, increasing the concentration polarization. This is generally referred to “flooding” phenomenon, which can raise concerns of durability and performance reduction due to reactant starvation. The GDL materials are usually rendered hydrophobic to facilitate liquid water drainage. Polytetrafluoroethylene (PTFE, a.k.a. DuPont’s Teflon™) is frequently adopted to modify the GDL wettability. Benzinger et al. [103] presented a study on the PTFE loading in various DM materials and their impacts on water transport. Sinha and Wang [104] used a pore-network model of GDLs, and found that liquid water preferentially flows through the connected hydrophilic pore network of a GDL with mixed wettability, see Fig. 17.



Mass flow at different portions of the GDL: $\bar{z} = 0.5$ (a); $\bar{z} = 0.75$ (b), \bar{z} is the dimensionless distance in z direction ranging from 0 to 1. The gray region denotes the solid with the light gray being the carbon fibers and the dark the binders. and liquid water distribution pattern from the drainage simulation (c)-(f).

Fig. 17

Pore-network models have also been employed by Gostick et al. [105]. A number of macroscopic models on two-phase flow have been developed to capture the two-phase characteristics in GDLs. They mostly treat the GDL as a uniform hydrophilic or hydrophobic medium. The capillary pressure is usually expressed as a function of saturation via the Leverett function in the literature, and the capillary-pressure gradient is expressed as a function of the saturation gradient. But it should be pointed out that the Leverett function was originally developed to describe liquid- water transport in soils; as such, it is not directly applicable to liquid-water transport in the GDLs of a PEM fuel cell due to their unique pore characteristics. To improve the multi-phase, particularly liquid, flow characteristics, the MPL can be added and placed between the GDL and CL. This layer is composed of carbon black powder with fine pore structure. Studies have showed that adding MPLs exhibit a better water drainage characteristics and fuel-cell performance. Gostick et al. indicated that the saturation in the GDL for water breakthrough is drastically reduced from ca. 25% to ca. 5% in the presence of MPL. Pasaogullari et al., Weber and Newman, Wang and Chen proposed that the MPL acts as a valve that drives water away from electrodes to reduce the electrode flooding [106-108]. At the MPL-GDL interface under certain conditions, the following relation was employed by Passagullari et al. [107] and Wang et al. [108]:

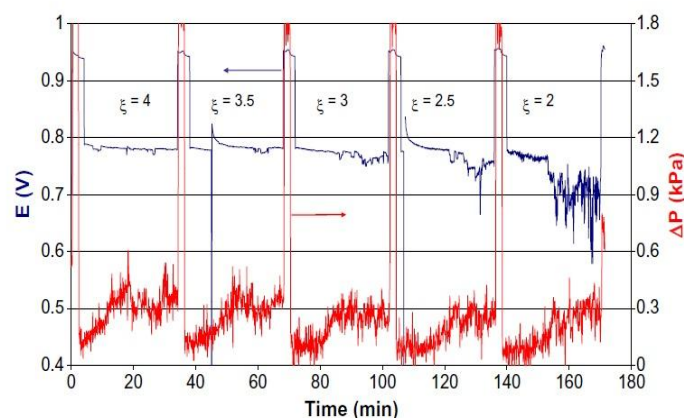
$$\sigma \cos(\theta_c^{GDL}) \left(\frac{\epsilon^{GDL}}{K^{GDL}} \right)^{1/2} J(s) = P_c^{GDL} = P_c^{MPL} = \sigma \cos(\theta_c^{MPL}) \left(\frac{\epsilon^{MPL}}{K^{MPL}} \right)^{1/2} J(s) \dots\dots\dots(9)$$

The above adopts the Leverett relation. Generally, the MPL porosity and mean pore-size are much smaller than that of the GDL. In their experimental efforts, Mukundan et al. and co-workers at LANL employed the neutron radiography to investigate the impacts of PTFE loadings on the water content within both GDLs and MPLs, and indicate that lower PTFE loadings in MPLs may show better performance and lower transport resistance. Hickner et al. also applied neutron imaging to quantify the liquid water content within MPLs and GDLs [109]. Though fundamental models have been developed to understand the liquid flow inside DMs, the newly experimental data from high-resolution neutron imaging indicate a big discrepancy with a model prediction [110]. In reality, the GDL is highly non-uniform in terms of its hydrophilic and hydrophobic properties; in other words, some areas in the GDL where carbon is present are highly hydrophilic whereas other areas where Teflon is present are highly hydrophobic, which is not accounted for in the current macroscopic approach. Further studies are needed in characterizing the pore-size distribution as well as hydrophilicity and hydrophobicity distributions and using this information to develop pore-level models. This type of work can aid in enabling realistic and accurate simulation of liquid water and gas transport through the GDLs with highly non-uniform pore-sizes and wettability and complete understanding how GDL properties influence fuel-cell performance. In addition, the macroscopic two-phase flow approach has been widely employed (see, e.g., Wang et al. [111], Natarajan and Nguyen [112], Mazumder and Cole [113]) to model liquid-water transport through the GDL and MPL. In this approach, capillary pressure is usually expressed as a function of saturation via the Leverett function [114]. In addition, GDLs may be subjected to degradation after long-term operations, such as wettability change due to PTFE loss and fiber breakage arising from freeze/thaw cycling. The surface properties were evaluated by Wood et al. [115] who presented single-fiber contact-angle and surface-energy data of a wide spectrum of GDL types to delineate the effects of hydrophobic post processing treatments [115]. Wood and

Borup further presented the cathode CL and GDL mass-transport overpotentials and analyzed the changes in a durability test [116]. They found little increase in the GDL mass-transport overpotential during the first period of about 500 h, but a substantial increase during the second period of approximately 500 h. Though Mukherjee et al. [117] presented a numerical study on the impact of GDL durability on fuel-cell performance, modeling degradation mechanisms is still lacking and remains a challenge at present, and thus requires further studies.

3.4. Gas flow channels, cooling channel, and bipolar plates

Gas flow channels (GFCs) are important components of PEM fuel cell and they supply and distribute hydrogen fuel and oxygen reactant for reactions and remove byproduct water. They are located within the bipolar plates with a typical cross-section dimension of around 1 mm. Insufficient supply of reactants will lead to hydrogen/oxygen starvation, reducing cell performance and durability. Bipolar plates (BP) provide mechanical support over DMs and conductive passages for both heat and electron transport. Fabrication of BPs, together with GFCs, may contribute an important portion of a fuel cell cost [1]. BP degradation, such as the metal plate corrosion and graphite crack, may happen and reduce fuel cell lifetime. Cooling channels can be machined within the bipolar plates, and is essential for the waste heat removal for large-scale fuel cell. Local hot spot formation can degrade the membrane and cause pin-hole or crack formation. Comprehensive reviews on flow fields and bipolar plates were provided by Wilkinson and Vanderleeden, EG&G Technical Service, and Li and Sabir [118-120]. In GFCs, partially or fully humidified hydrogen and air are injected into anode and cathode, respectively. Several types of flow fields have been developed, they are parallel, serpentine, pin-type, interdigitated, and porous media designs. A zigzag flow field with different aspect ratio has also been proposed and studied [121]. Jeon et al. [122] investigated single channel, double channel, cyclic-single channel, and symmetric-single channel patterns, and found that fuel-cell performance varies in different configurations. Karvonen et al. [123] numerically investigated parallel channel flows and developed a strategy for a small variation (2%) of flow velocity among channels. Perng et al. [124] indicated that a rectangular cylinder installed transversely in the flow channel can enhance fuel-cell performance. Perng and Wu [125] showed that baffle blockage in tapered channels provides a better convection and a higher fuel flow velocity and enhances cell performance. Several studies also investigated the cross-section dimension of GFCs. Inoue et al. examined channel height and found that shallow channels may enhance oxygen transport to electrodes. Wang [126] analyzed the channel in-plane dimension by examining heat and electron transport characteristics. Wang et al. [127] investigated the channel aspect ratio for serpentine flow field. Convection is the dominant force for species transport in a GFC, and the flow has been customarily treated using the single-phase approach: either considering the vapor phase as superly saturated or treating it as mist flow – neither of these two approaches describe reality of flow in GFCs. The streams frequently fall in the two-phase regime due to water addition from the ORR. Liquid may block channels, hampering reactant supply and unstable fuel cell operation.

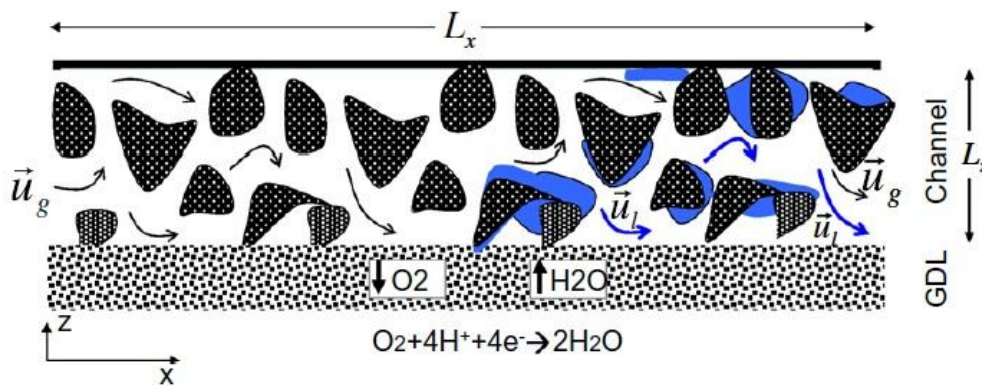


Cell voltage variation with time for different air stoichiometric ratios (current density = 0.2 A/cm², anode/cathode RH = 70%, temperature = 80 °C, back pressure = 150 kPa).

Fig. 18

Fig.18 shows cell voltage variation over time (the blue1 or higher trace) for five different air stoichiometric ratios (n) at the current density of 0.2 A/cm² in a 14 cm² PEM fuel cell. It can be seen that the cell voltage becomes oscillatory with a magnitude of 120 mV at the stoichiometry of 2. Thus, cathodeflooding results in a performance loss (120 mV) that completely negates any potential improvement from catalyst

development: for instance, a 4-fold increase in catalytic activity yields only 45 mV gain in cell voltage. Moreover, the voltage fluctuation induced by channel flooding may set up a voltage cycling at high potentials, which could result in serious durability issues. Due to the important role of liquid water in the channel flow, the wettability of the GFC wall, i.e. the hydrophilicity or hydrophobicity, may have great impacts on the channel two-phase flow: hydrophilic GFC walls seem to be favored by practitioners since they facilitate the formation of a thin liquid-water film and provide a steady flow of air (and thus O₂) to reaction sites, whereas the hydrophobic GFC walls can result in unsteady PEMFC operation. Modeling the channel two-phase flow in fuel cell is numerically very challenging. Wang et al. envisaged the mini-channels as structured and ordered porous media. A two-phase channel flooding model was developed based on the two-phase mixture description. Three fundamental issues critical to the channel design are explained, they are water buildup, channel heterogeneity, and flow maldistribution. Basu et al. [128,129] also developed a two-phase model to study the flow maldistribution in fuel cell channels. Wang further proposed a concept of porous-media channels, see Fig. 19, and examined the characteristics of reactant flows, heat transfer, species transport, and two-phase transport. Liquid profile along the channel was analytically obtained using a two-fluid flow model. Several studies were conducted to investigate the liquid transport using the volume of fluid (VOF) and LB (Lattice Boltzmann) methods [130].



Configuration of a porous media channel and schematic of the internal two-phase flow

Fig 19

Most of them focused on the dynamics of liquid droplets, which will be detailed in the next sub-section. However, modeling two-phase behavior in channels that can be incorporated to a full fuel cell model still remains as a challenge due to lack of efficient numerical methods to track the two-phase interface and capture multi-component transport. Further study is required to characterize the two-phase flow in the full regime of fuel cell operation such as slug and slug-annulus transition. Also models fully couples the channel two-phase flow, transport in the porous DM, and the electrochemical reaction kinetics in the MEA are highly needed. The bipolar plates (BPs) contribute a primary portion of fuel cell weight. The DOE target on the BP weight is <0.4 kg/kW by 2015 and Adrianowycz showed their development status in 2009 is 0.57 kg/kW [228]. A popular BP material is the non-porous graphite, which is chemically stable and highly conductive to electrons and heat. Cooling channels must be added to keep fuel cells at their optimal temperature when a large amount of waste heat is generated. Cooling channel designs have been received relatively small attention in past comparing with other components. Wang and Wang shows the cooling channel design and control can be optimized for better water/thermal management [131]. Yu et al. and Inoue et al. also presented a study on cooling channels or units for PEM fuel cell [132,133].

3.5. GDL/GFC interface

At the cathode GDL/GFC interface, oxygen transports towards the electrode where it reacts with protons and electrons to produce water, which eventually enters the channel. The interfacial resistance for reactant transport will be significantly increased due to the presence of liquid water. Optical visualizations, see Fig. 20, showed that liquid water exists as droplets on the GDL surface, taken away by the gas flow or attach to the channel wall.

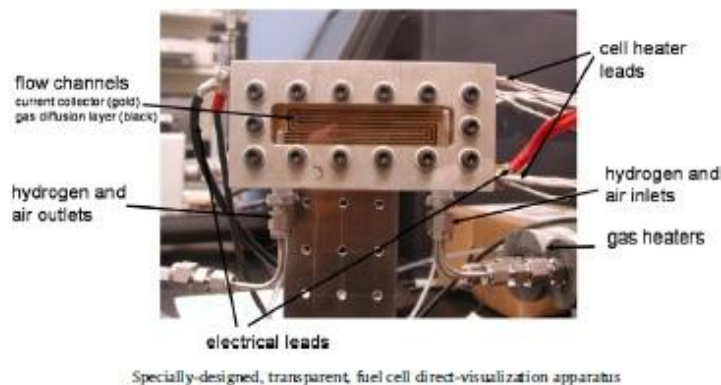


Fig.20 Flow visualization apparatus for PEMFC

The behavior of liquid water droplets at the GDL/GFC interface consists of three sub-processes: (1) transport from the catalyst layer to the GDL/GFC interface via capillary action; (2) removal at the GDL/GFC interface via detachment or evaporation; and (3) transport through the GFC in form of films, droplets and/or vapor. The growth and detachment of water droplets are influenced by two factors: the operating conditions of the fuel cell and the physical (e.g., surface roughness) and chemical (e.g., wettability) material characteristics of the GDL surface (e.g. in terms of the hydrophilic/hydrophobic properties). Chen et al. [134] pioneered the analysis of droplet instability and detachment and they indicated that the static contact angle (θ_s) and contact angle hysteresis (the difference between advancing and receding contact angles, i.e., $\theta_A - \theta_R$), are both important parameters in determining the force required to move a droplet across a surface.

In addition, the VOF-based modeling has also been conducted to investigate the droplet dynamics at the interface. The droplets on the GDL surface increases reactant transport resistance into the GDL as well as liquid flow inside. Meng and Wang and Wang et al. used liquid coverage to account for the droplet presence in their study [135]. Further work of interests includes development of 3D fundamental models to predict droplet behaviors at the interface, particularly the impact of GDL surface properties on droplet dynamics. Given the droplets appear randomly at the GDL surface, statistical methods might be adopted to evaluate the portion of area covered by liquid. Also the GFC–GDL interface bridges the transport in channels and GDL, therefore a fundamental understanding of this connection and a mathematical model that can describe the connection will be highly needed. Further detailed study on more realistic droplet emerging/detachment in a real fuel cell channel, a wide range of regimes, as well as its coupling with the transport and electrochemical reaction is highly needed.

3.6. Stack

A single fuel cell is only able to produce a certain voltage and current. In order to obtain a higher voltage and current or power, fuel cells are connected in either series or parallel, called stacks, see Fig. 22. At the stack level, water and heat management becomes more complex due to the interactions of constituent sub-cells. Individual cells communicate in many ways in a stack. One is the electrical connection, i.e. the electrical current flows through all the individual cells in a series stack, therefore a local high electronic resistance will significantly affect the stack performance.



A 5 kW fuel cell manufactured by PlugPower (large cell), 25 W fuel cell (three cell stack) manufactured by H2ECONomy (smaller silver cell), 30 W fuel cell manufactured by Avista Labs

Fig.22

Another one is through flow field. In practice, several fuel cells share one inlet/ outlet manifold in a stack. Therefore, a fuel cell with high flow resistance receives fewer amounts of the reactants, causing local reactant starvation (which further leads to cell performance decay and material degradation). A third one is heat transfer connection. A fuel cell exhibiting a larger thermal resistance or exposing to insufficient cooling will be subject to a higher temperature and dispose its extra waste heat to neighboring fuel cells. Such local hot fuel cell may reduce cell performance and raise concerns of material degradation. Detailed fundamental study at the stack level becomes challenging. Most studies only considered a simplified stack model, e.g. Promislow and Wetton [136] developed a model of steady-state thermal transfer in stacks. The model is appropriate for straight coolant channel unit cell designs and considers quantities averaged over the cross-channel direction, ignoring the impact of the gas and coolant channel geometries. Kim et al. [137] developed an electrical interaction model for stacks and validated it using two types of anomalies. The unit cells are described by simple, steady-state, 1 + 1-dimensional models appropriate for straight reactant gas channel designs. Berg et al. [138] also presented a similar stack approach with the unit cells described by one dimensional models appropriate for straight reactant gas channel designs. Karimi et al. used a flow network to determine the pressure and flow distributions [139]. The results were incorporated into the individual cell model developed by Baschuk and Li [140]. Chang et al. used a flow distribution model to examine the sensitivity of stack performance to operating conditions (inlet velocity and pressure) and design parameters (manifold, flow configuration and friction factor). Park and Li presented a flow model and concluded that flow uniformity can be enhanced by a large manifold. Chang et al. developed a stack model incorporating flow distribution effects and a reduced-dimension unit cell model. The mass and momentum conservation are applied throughout the stack. Flow splitting and recombination are considered at each tee junction, while along the unit cell channels, reactant consumption and byproduct production are accounted for. Yu et al. proposed a water and thermal management model of a Ballard fuel cell stack which takes a set of gas input conditions and stack parameters such as channel geometry, heat transfer coefficients, and operating current [141]. The model can be used to optimize the stack thermal and water management. Chen et al. numerically investigated the flow distribution in a stack, and concluded that the channel resistance, manifold dimension and gas feed rate may affect flow distributions [142]. Chang et al. [143] proposed separation of the complex model into computationally manageable pieces. The computational method is backed by some simplified analysis and a convergence study. At the stack level, the following issues are also considered as important areas requiring further study: they are optimization of stack system (e.g. stack design and reactant manifold); fuel processing subsystem (fuel management, reformer, steam generator, shift reactor, etc); power and electric subsystem; thermal management subsystem (cooling, heat exchanger); and ancillary subsystem (air supply, water treatment, safety, monitoring, ventilation fans, misc). Modeling and simulation of PEM fuel cell stacks provide a powerful tool for stack design and optimization. Comprehensive models that fully couple the reactant flow in the GFC and manifolds and the transport within fuel cell in conjunction with electrochemical reaction are highly needed. One critical part is the two-phase flow in the complex flow field of stacks, which is essential to capture the flow maldistribution phenomena. In addition, computational studies based on a

comprehensive model are still computationally too expensive at current so efficient numerical schemes are in need.

IV. Summary and concluding remarks

The latest status of PEM fuel cell technology and its applications has been reviewed, and the needs on fundamental research have been discussed. PEM fuel cells have the potentials to reach 60% in electrical energy conversion or overall 80% in co-generation of electrical and thermal energies with >90% reduction in major pollutants. The following three major PEMFC applications were discussed, i.e. automobile, portable, and stationary applications. To date, approximately 75,000 fuel cells have been shipped worldwide and during the last year alone about 24,000 fuel cells were shipped. Two primary barriers to the world-wide commercialization of PEM fuel cell technology were explained: durability and cost. To further overcome the barriers to the wide deployment of fuel cells, fundamental breakthroughs are needed. This review briefly discusses the role and summarizes the needs on fundamental research as well as the associated challenges. Aspects of materials development, acquisition of fundamental knowledge, and development of analytical models and experimental tools are required. Improvement on catalyst, MEA components, and bipolar plates are particularly important for overcoming the two major commercialization barriers (i.e., durability and cost). Specially, for membrane and catalyst layer (which consist of the MEA), both require significant further research in order to identify and develop alternative cost-effective materials. Correlations of membrane properties to performance for general polymer electrolyte materials are much in need. For GDLs and MPLs, fundamental understanding of liquid-water behaviors in these components is required, in particular on the effects of the micro structure of the media and the proper combination of hydrophobicity and hydrophilicity. For bipolar plates and GFCs, advanced fabrication methods are needed to reduce the cost of the plates and improve their corrosion resistance. Lastly, fundamental knowledge of liquid droplet removal at the GDL/GFC interfaces and two-phase flow in micro-/mini-channels is challenging to obtain, but such knowledge is in great urgent need in order to develop optimized GDL materials and GFC designs that can ensure efficient water removal and reactant supply and avoid flow maldistribution and thus maintain high fuel-cell performance.

References

- [1] Papageorgopoulos D. DOE fuel cell technology program overview and introduction to the 2010 fuel cell pre-solicitation workshop in DOE fuel cell pre-solicitation workshop. Department of Energy, Lakewood, Colorado; 2010.
- [2] Wand G. Fuel cell history, Part One. 14.
- [3] Appleby AJ, Yeager EB. Solid polymer electrolyte fuel cells (SPEFCs). *Energy* 1986;11(1-2):137-52.
- [4] Gittleman C, DM, Jorgensen S, Waldecker J, Hirano S, Mehall M. Automotive fuel cell R&D needs. In: DOE fuel cell pre-solicitation workshop. Department of Energy, Lakewood, Colorado; 2010.
- [5] Garche J, Jorissen L. PEMFC fuel cell. In: Vielstich W, Gasteiger H, Lamm A, editors. *Handbook of fuel cells: fundamentals, technology and applications*. John Wiley & Sons, Ltd.; 2003.
- [6] Zhang S et al. A review of accelerated stress tests of MEA durability in PEM fuel cells. *Int J Hydrogen Energy* 2009;34(1):388-404.
- [7] Borup R, et al. PEM fuel cell durability. 2008 DOE hydrogen program review June 9-13, 2008, 5. <http://www.hydrogen.energy.gov/pdfs/review08/fc_26_borup.pdf>.
- [8] Schmittinger W, Vahidi A. A review of the main parameters influencing long term performance and durability of PEM fuel cells. *J Power Sources* 2008;180(1):1-14.
- [9] Borup R et al. Scientific aspects of polymer electrolyte fuel cell durability and degradation. *Chem Rev* 2007;107(10):3904-51.
- [10] Wood DL, Borup RL. In: Buchi MIFN, Schmidt TJ, editors. *Polymer electrolyte fuel cell durability*. New York: Springer; 2009. P. 159.
- [11] Directed technologies I. Mass production cost estimation for direct H₂ PEM fuel cell systems for automotive applications: 2008 update 2009. p. 10.
- [12] Lipman T, Sperling D. Market concepts, competing technologies and cost challenges for automotive and stationary applications. In: Vielstich W, Gasteiger H, Lamm A, editors. *Handbook of fuel cells: fundamentals, technology and applications*. John Wiley & Sons, Ltd.; 2003. p. 1318-28.
- [13] Stumper J, Stone C. Recent advances in fuel cell technology at Ballard. *J Power Sources* 2008;176(2):468-76.
- [14] Jerram LC. 2008 Bus survey. *Fuel Cell Today* 2008.
- [15] Adamson K-A, Jerram LC. 2009 Niche transport survey. *Fuel Cell Today* 2009:11-2.
- [16] Hwang JJ, Wang DY, Shih NC. Development of a light weight fuel cell vehicle. *J Power Sources* 2005;141(1):108-15.
- [17] Butler J. Portable fuel cell survey 2009. *Fuel Cell Today* 2009.
- [18] Narayanan SR, Valdez TI, Rohatgi N. Portable direct methanol fuel cell system. In: Vielstich W, Gasteiger HA, Lamm A, editor. *Handbook of fuel cells*. John Wiley and Sons; 2003.
- [19] Hayase M, Kawase T, Hatsuzawa T. Miniature 250 lm thick fuel cell with monolithically fabricated silicon electrodes. *Electrochem Solid-State Lett* 2004;7(8):A231-4.
- [20] Lee S-J, Chen Y-P, Huang C-H. Electroforming of metallic bipolar plates with micro-featured flow field. *J Power Sources* 2005;145(2):369-75.
- [21] Ito T, Kaneko S, Kunimatsu M. Fabrication and characterization of a thin l- PEMFC with microfabricated grooves on electroformed current collector plate. *Electrochem Solid-State Lett* 2009;12(11):B154-7.

- [22] Hahn R et al. Development of a planar micro fuel cell with thin film and micro patterning technologies. *J Power Sources* 2004;131(1-2):73-8.
- [23] Hsieh SS et al. *J Solid State Electrochem* 2005;9:121-31.
- [24] Cha SW et al. The scaling behavior of flow patterns: a model investigation. *J Power Sources* 2004;134(1):57-71.
- [25] Park BY, Madou MJ. Design, fabrication, and initial testing of a miniature PEM fuel cell with micro-scale pyrolyzed carbon fluidic plates. *J Power Sources* 2006;162(1):369-79.
- [26] Lin P-C, Park BY, Madou MJ. Development and characterization of a miniature PEM fuel cell stack with carbon bipolar plates. *J Power Sources* 2008;176(1):207-14.
- [27] Wang Y et al. Fabrication and characterization of micro PEM fuel cells using pyrolyzed carbon current collector plates. *J Power Sources* 2010.
- [28] Henriques T, César B, Branco PJC. Increasing the efficiency of a portable PEM fuel cell by altering the cathode channel geometry: a numerical and experimental study. *Appl Energy* 2010;87(4):1400-9.
- [29] Plug power wins award to operate GenSys units in NY homes. *Fuel Cells Bull* 2009; 2009(9): 6-6.
- [30] Plug power, SFO technologies sign GenSys manufacture, supply deal for India. *Fuel Cells Bull* 2009; 2009(12): 9-9.
- [31] Ballard. PEM fuel cell product portfolio; 2009.
- [32] Gurau V, Mann JA. A critical overview of computational fluid dynamics multiphase models for proton exchange membrane fuel cells. *SIAM J Appl Math* 2009;70(2):410-54.
- [33] Wang C-Y. Fundamental models for fuel cell engineering. *Chem Rev* 2004;104(10):4727-66.
- [34] Siegel C. Review of computational heat and mass transfer modeling in polymer-electrolyte-membrane (PEM) fuel cells. *Energy* 2008;33(9):1331-52.
- [35] Djilali N. Computational modelling of polymer electrolyte membrane (PEM) fuel cells: challenges and opportunities. *Energy* 2007;32(4):269-80.
- [36] Wang Y, Basu S, Wang CY. Modeling two-phase flow in PEM fuel cell channels. *J Power Sources* 2008;179(2):603-17.
- [37] Ma Y-L et al. Conductivity of PBI membranes for high-temperature polymer electrolyte fuel cells. *J Electrochem Soc* 2004;151(1):A8-A16.
- [38] Zhang J et al. High temperature PEM fuel cells. *J Power Sources* 2006;160(2):872-91.
- [39] Smitha B, Sridhar S, Khan AA. Solid polymer electrolyte membranes for fuel cell applications – a review. *J Membrane Sci* 2005;259(1-2):10-26.
- [40] Arcella V et al. Membrane electrode assemblies based on perfluorosulfonic ionomers for an evolving fuel cell technology. *Desalination* 2006;199(1-3):6-8.
- [41] Merlo L et al. Membrane electrode assemblies based on HYFLON ion for an evolving fuel cell technology – separation science and technology. *SeparatSci Technol* 2007;42(13):2891-908.
- [42] Li Q et al. High temperature proton exchange membranes based on polybenzimidazoles for fuel cells. *ProgPolymSci* 2009;34(5):449-77.
- [43] Atkinson S. Membranes for fuel cells compared in real time. *Membrane Technol* 2005;2005(1):5-7.
- [44] Gierke TD, Hsu WY. Perfluorinated ionomer membranes. In: Eisenberg A, Yeager HL, editors. ACS symposium series No.180. American Chemical Society: Washington, DC; 1982.
- [45] Kreuer KD, Rabenau A, Weppner W. Vehicle mechanism, a new model for the interpretation of the conductivity of fast proton conductors. *AngewChemIntEdEngl* 1982;21:208-9.
- [46] Kornyshev AA, Kuznetsov AM, Spohr E, Ulstrup J. Kinetics of proton transport in water. *J PhysChem B* 2003;107:3351-66.
- [47] Marx D et al. The nature of the hydrated excess proton in water. *Nature* 1999;397(6720):601-4.
- [48] Springer TE, Zawodzinski TA, Gottesfeld S. Polymer electrolyte fuel cell model. *J Electrochem Soc* 1991;138(8):2334-42.
- [49] Cappadonia M, Erning JW, Stimming U. Proton conduction of Nafion₁₁₇ membrane between 140 K and room temperature. *J ElectroanalChem* 1994;376(1-2):189-93.
- [50] Wang Y, Mukherjee PP, Mishler J, Mukundan R, Borup RL. Cold start of polymer electrolyte fuel cells: three-stage startup characterization. *ElectrochimActa* 2010;55:2636-44.
- [51] Thompson EL et al. Investigation of low-temperature proton transport in Nafion using direct current conductivity and differential scanning calorimetry. *J Electrochem Soc* 2006;153(12):A2351-62.
- [52] Cappadonia M et al. Conductance of Nafion 117 membranes as a function of temperature and water content. *Solid State Ionics* 1995;77:65-9.
- [53] Conductivity in polymer electrolytes. In: ASME proceedings of IMECE'04, paper #60848; 2004.
- [54] Ise M, Kreuer KD, Maier J. Electroosmotic drag in polymer electrolyte membranes: an electrophoretic NMR study. *Solid State Ionics* 1999;125(1-4):213-23.
- [55] Zawodzinski Jr TA et al. Characterization of polymer electrolytes for fuel cell applications. *Solid State Ionics* 1993;60(1-3):199-211.
- [56] Fuller TF, Newman J. Experimental determination of the transport number of water in Nafion 117 membrane. *J Electrochem Soc* 1992;139(5):1332-7.
- [57] Xie G, Okada T. Water transport behavior in Nafion 117 membranes. *J Electrochem Soc* 1995;142(9):3057-62.
- [58] Ge S, Yi B, Ming P. Experimental determination of electro-osmotic drag coefficient in Nafion membrane for fuel cells. *J Electrochem Soc* 2006;153(8):A1443-50.
- [59] Ye X, Wang C-Y. Measurement of water transport properties through membrane-electrode assemblies. *J Electrochem Soc* 2007;154(7):B676-82.
- [60] Adachi M et al. Correlation of in situ and ex situ measurements of water permeation through Nafion NRE211 proton exchange membranes. *J Electrochem Soc* 2009;156(6):B782-90.
- [61] Bernardi DM, Verbrugge MW. A mathematical model of the solid-polymer electrolyte fuel cell. *J Electrochem Soc* 1992;139(9):2477-91.
- [62] Büchi FN, Wakizoe M, Srinivasan S. Microelectrode investigation of oxygen permeation in perfluorinated proton exchange membranes with different equivalent weights. *J Electrochem Soc* 1996;143:927-32.

- [63] Zawodzinski TA et al. The water content dependence of electro-osmotic drag in proton-conducting polymer electrolytes. *ElectrochimActa*1995;40(3):297–302.
- [64] Chen KS et al. Final report on LDRD project: elucidating performance of proton-exchange-membrane fuel cells via computational modeling with experimental discovery and validation, in SAND2006-6964, Sandia Technical Report; 2006.
- [65] Chen KS, Hickner MA. A new constitutive model for predicting proton conductivity in polymer electrolytes. In: Proceedings of 2004 international mechanical engineering congress and exhibits; 2004.
- [66] Weber AZ, Newman J. Transport in polymer-electrolyte membranes. *J ElectrochemSoc* 2003;150(7):A1008–15.
- [67] Weber AZ, Newman J. Transport in polymer-electrolyte membranes. *J ElectrochemSoc* 2004;151(2):A311–25.
- [68] Yu P, Pemberton M, Plasse P. PtCo/C cathode catalyst for improved durability in PEMFCs. *J Power Sources* 2005;144(1):11–20.
- [69] Rao CRK, Trivedi DC. Chemical and electrochemical depositions of platinum group metals and their applications. *CoordChem Rev* 2005;249(5–6):613–31.
- [70] Wells P et al., Preparation of Cr/Pt/C catalysts by the controlled surface modification of Pt/C using an organometallic precursor. In: 3rd European PEFC forum, Lucerne, Switzerland; 2005.
- [71] Debe MK. Advanced cathode catalysts and supports for PEM fuel cells. In: 2010 Hydrogen program annual merit review and peer evaluation meeting. Washington, DC; 2010.
- [72] Vante NA, Tributsch H. Energy conversion catalysis using semiconducting transition metal cluster compounds. *Nature* 1986;323:431–2.
- [73] Fernandez JL et al. Pd–Ti and Pd–Co–Au electrocatalysts as a replacement for platinum for oxygen reduction in proton exchange membrane fuel cells. *J Am ChemSoc* 2005;127(38):13100–1.
- [74] Bashyam R, Zelenay P. A class of non-precious metal composite catalysts for fuel cells. *Nature* 2006;443(7107):63–6.
- [75] Zelenay P. Advanced cathode catalysts. In: 2010 Hydrogen program annual merit review and peer evaluation meeting, Washington, DC; 2010.
- [76] Eisman et al. Separators and ion-exchange membranes. *ElectrochemSocProc*1986;86(13):186.
- [77] Gottesfeld S, Pafford J. A new approach to the problem of carbon monoxide poisoning in fuel cells operating at low temperatures. *J ElectrochemSoc*1988;135(10):2651–2.
- [78] Dhathathreyan KS, Rajalakshmi N. Polymer electrolyte membrane fuel cell. AnamayaPublishers; 2006.
- [79] Siegel NP. Development and validation of a computational model for a proton exchange membrane fuel cell. In: Ph.D. dissertation. Virginia Polytechnic Institute and State University: Blacksburg, VA; 2003.
- [80] Siegel NP et al. Single domain PEMFC model based on agglomerate catalyst geometry. *J Power Sources* 2003;115(1):81–9.
- [81] Harvey D. Three-dimensional CFD model for PEFC cathodes: application to serpentine flow fields, in fuel cell research centre. Kingston (Ontario): Queen’s University; 2006.
- [82] Harvey D, Pharoah JG, Karan K. A comparison of different approaches to modeling the PEMFC catalyst layer. *J Power Sources* 2008;179(1):209–19.
- [83] Marr C, Li X. Composition and performance modelling of catalyst layer in a proton exchange membrane fuel cell. *J Power Sources* 1999;77(1):17–27.
- [84] Schwarz DH, Djilali N. 3D modeling of catalyst layers in PEM fuel cells. *J ElectrochemSoc* 2007;154(11):B1167–78.
- [85] Shah AA et al. Transient non-isothermal model of a polymer electrolyte fuel cell. *J Power Sources* 2007;163(2):793–806.
- [86] Mathias M et al. Handbook of fuel cells: fundamentals. In: Vielstich W, Gasteiger H, Lamm A, editors. Technology and applications. John Wiley & Sons, Ltd.; 2003.
- [87] Larminie J, Dicks A. Fuel cell systems explained. John Wiley & Sons; 2000.
- [88] Yi JS, Nguyen TV. Multicomponent transport in porous electrodes of proton exchange membrane fuel cells using the interdigitated gas distributors. *J ElectrochemSoc* 1999;146(1):38–45.
- [89] Wang Y, Wang C-Y. Simulation of flow and transport phenomena in a polymer electrolyte fuel cell under low-humidity operation. *J Power Sources* 2005;147(1–2):148–61.
- [90] Dutta S, Shimpalee S, Van Zee JW. Three-dimensional numerical simulation of straight channel PEM fuel cells. *J ApplElectrochem* 2000;30(2):135–46.
- [91] Wang Y, Wang C-Y. Modeling polymer electrolyte fuel cells with large density and velocity changes. *J ElectrochemSoc* 2005;152(2):A445–53.
- [92] Mazumder S, Cole JV. Rigorous 3-D mathematical modeling of PEM fuel cells. *J ElectrochemSoc* 2003;150(11):A1503–9.
- [93] Hwang JJ. Thermal-electrochemical modeling of a proton exchange membrane fuel cell. *J ElectrochemSoc* 2006;153(2):A216–24.
- [94] Wang Y, Wang C-Y, Nonisothermal A. Two-phase model for polymer electrolyte fuel cells. *J ElectrochemSoc* 2006;153(6):A1193–200.
- [95] Nam JH, Kaviany M. Effective diffusivity and water-saturation distribution in single- and two-layer PEMFC diffusion medium. *Int J Heat Mass Transfer* 2003;46(24):4595–611.
- [96] Meng H, Wang C-Y. Electron transport in PEFCs. *J ElectrochemSoc*2004;151(3):A358–67.
- [97] Wang Y et al. Stochastic modeling and direct simulation of the diffusion media for polymer electrolyte fuel cells. *Int J Heat Mass Transfer* 2010;53(5–6):1128–38.
- [98] Schulz VP et al. Numerical evaluation of effective gas diffusivity – saturation dependence of uncompressed and compressed gas diffusion media in PEFCs. *ECS Trans* 2006;3(1):1069–75.
- [99] Sinha PK, Mukherjee PP, Wang C-Y. Impact of GDL structure and wettability on water management in polymer electrolyte fuel cells. *J Mater Chem*2007;17(30):3089–103.
- [100] Mukherjee PP, Wang C-Y, Kang Q. Mesoscopic modeling of two-phase behavior and flooding phenomena in polymer electrolyte fuel cells. *ElectrochimActa* 2009;54(27):6861–75.
- [101] Becker J, Schulz V, Wiegmann A. Numerical determination of two-phase material parameters of a gas diffusion layer using tomography images. *J Fuel Cell SciTechnol* 2008;5(2):021006.
- [102] Becker J et al. Determination of material properties of gas diffusion layers: experiments and simulations using phase contrast tomographic microscopy. *J ElectrochemSoc* 2009;156(10):B1175–81.
- [103] Benziger J et al. Water flow in the gas diffusion layer of PEM fuel cells. *J Membrane Sci* 2005;261(1–2):98–106.

- [104] Sinha PK, Wang CY. Liquid water transport in a mixed-wet gas diffusion layer of a polymer electrolyte fuel cell. *ChemEngSci* 2008;63(4):1081–91.
- [105] Gostick JT et al. Pore network modeling of fibrous gas diffusion layers for polymer electrolyte membrane fuel cells. *J Power Sources* 2007;173(1):277–90.
- [106] Weber AZ, Newman J. Effects of microporous layers in polymer electrolyte fuel cells. *J ElectrochemSoc* 2005;152(4):A677–88.
- [107] Pasaogullari U, Wang C-Y, Chen KS. Two-phase transport in polymer electrolyte fuel cells with bilayer cathode gas diffusion media. *J ElectrochemSoc* 2005;152(8):A1574–82.
- [108] Wang Y, Chen KS. In: Proceedings of the 8th International fuel cell science, engineering & technology conference, Brooklyn, NY; 2010.
- [109] Hickner MA et al. In situ high-resolution neutron radiography of crosssectional liquid water profiles in proton exchange membrane fuel cells. *J ElectrochemSoc* 2008;155(4):B427–34.
- [110] Borup R. FC-35: water transport exploratory studies. In: Energy Do, editor. Hydrogen program review; 2009.
- [111] Wang ZH, Wang CY, Chen KS. Two-phase flow and transport in the air cathode of proton exchange membrane fuel cells. *J Power Sources* 2001;94(1):40–50.
- [112] Natarajan D, Nguyen TV. A two-dimensional, two-phase, multicomponent, transient model for the cathode of a proton exchange membrane fuel cell using conventional gas distributors. *J ElectrochemSoc* 2001;148(12):A1324–35.
- [113] Mazumder S, Cole JV. Rigorous 3-D mathematical modeling of PEM fuel cells. *J ElectrochemSoc* 2003;150(11):A1510–7.
- [114] Leverett MC. Capillary behavior in porous solids. *Trans AIME* 1941;142:151–69.
- [115] Wood DL, Rulison C, Borup RL. Surface properties of PEMFC gas diffusion layers. *J ElectrochemSoc* 2010;157(2):B195–206.
- [116] Wood DL, Borup IRL. Estimation of mass-transport overpotentials during long-term PEMFC operation. *J ElectrochemSoc* 2010;157(8):B1251–62.
- [117] Mukherjee PP, Mukundan R, Borup RL. Modeling of durability effect on the flooding behavior in the PEFC gas diffusion layer. In: Proceedings of ASME fuel cell 2010, 8th ASME international fuel cell science, engineering, and technology conference; 2010.
- [118] Wilkinson DP, Vanderleeden O. Handbook of fuel cells: fundamentals. In: Vielstich W, Gasteiger H, Lamm A, editors. Technology and applications. John Wiley & Sons, Ltd.; 2003 [chapter 27].
- [119] EG&G Technical Services I. Fuel cell handbook, vol. 7. 2004: US Department of Energy, Office of Fossil Energy, National Energy Technology Laboratory.
- [120] Li X, Sabir I. Review of bipolar plates in PEM fuel cells: flow-field designs. *Int J Hydrogen Energy* 2005;30(4):359–71.
- [121] Jiang F et al. Simulation of a PEMFC with zigzag flow field. In: ASME eighth international fuel cell science, engineering & technology conference, Brooklyn, NY; 2010.
- [122] Jeon DH et al. The effect of serpentine flow-field designs on PEM fuel cell performance. *Int J Hydrogen Energy* 2008;33(3):1052–66.
- [123] Karvonen S et al. Modeling of flow field in polymer electrolyte membrane fuel cell. *J Power Sources* 2006;161(2):876–84.
- [124] Perng S-W et al. Numerical predictions of a PEM fuel cell performance enhancement by a rectangular cylinder installed transversely in the flow channel. *Appl Energy* 2009;86(9):1541–54.
- [125] Perng S-W, Wu H-W. Non-isothermal transport phenomenon and cell performance of a cathodic PEM fuel cell with a baffle plate in a tapered channel. *Appl Energy* 2010;88(1):52–67.
- [126] Wang Y. Porous-media flow fields for polymer electrolyte fuel cells. *J ElectrochemSoc* 2009;156(10):B1134–41.
- [127] Wang X-D et al. Channel aspect ratio effect for serpentine proton exchange membrane fuel cell: role of sub-rib convection. *J Power Sources* 2009;193(2):684–90.
- [128] Basu S, Li J, Wang C-Y. Two-phase flow and maldistribution in gas channels of a polymer electrolyte fuel cell. *J Power Sources* 2009;187(2):431–43.
- [129] Basu S, Wang C-Y, Chen KS. Two-phase flow maldistribution and mitigation in polymer electrolyte fuel cells. *J Fuel Cell Sci Technol* 2009;6(3):031007.
- [130] Hao L, Cheng P. Lattice Boltzmann simulations of anisotropic permeabilities in carbon paper gas diffusion layers. *J Power Sources* 2009;186(1):104–14.
- [131] Wang Y, Wang C-Y. Ultra large-scale simulation of polymer electrolyte fuel cells. *J Power Sources* 2006; 153(1):130–5.
- [132] Yu SH et al. Numerical study to examine the performance of multi-pass serpentine flow-fields for cooling plates in polymer electrolyte membrane fuel cells. *J Power Sources* 2009;194(2):697–703.
- [133] Inoue G et al. Numerical analysis of relative humidity distribution in polymer electrolyte fuel cell stack including cooling water. *J Power Sources* 2006;162(1):81–93.
- [134] Chen KS, Hickner MA, Noble DR. Simplified models for predicting the onset of liquid water droplet instability at the gas diffusion layer/gas flow channel interface. *Int J Energy Res* 2005;29(12):1113–32.
- [135] Meng H, Wang C-Y. Model of two-phase flow and flooding dynamics in polymer electrolyte fuel cells. *J ElectrochemSoc* 2005;152(9):A1733–41.
- [136] Promislow K, Wetton B. A simple, mathematical model of thermal coupling in fuel cell stacks. *J Power Sources* 2005;150:129–35.
- [137] Kim GS et al. Electrical coupling in proton exchange membrane fuel cell stacks. *J Power Sources* 2005;152:210–7.
- [138] Berg P et al. Electrical coupling in proton exchange membrane fuel cell stacks: mathematical and computational modelling. *IMA J Appl Math* 2006;71(2):241–61.
- [139] Karimi G, Baschuk JJ, Li X. Performance analysis and optimization of PEM fuel cell stacks using flow network approach. *J Power Sources* 2005;147(1-2):162–77.
- [140] Baschuk JJ, Li X. Mathematical model of a PEM fuel cell incorporating CO poisoning and O₂ (air) bleeding. *Int J Global Energy Issues* 2003;20(3):245–76.
- [141] Yu X, Zhou B, Sobiesiak A. Water and thermal management for Ballard PEM fuel cell stack. *J Power Sources* 2005;147(1-2):184–95.
- [142] Chen C-H, Jung S-P, Yen S-C. Flow distribution in the manifold of PEM fuel cell stack. *J Power Sources* 2007;173(1):249–63.
- [143] Chang P et al. Reduced dimensional computational models of polymer electrolyte membrane fuel cell stacks. *J Computat Phys* 2007;223(2):797–821.